ABSTRACT

FLEMING III, JOHN T. Characteristic Methods for Solving the Particle Transport Equation in 1-D Spherical Geometry. (Under the direction of Dmitriy Y. Anistratov.)

A family of numerical methods for solving the particle transport equation in 1-D spherical geometry are developed using the method of characteristics. The development of these methods is driven by a desire to: (i) provide solutions to transport problems which cannot otherwise be determined using analytic techniques (ii) provide comparative solutions to test methods developed for other curvilinear geometries and (iii) develop methods for RZ geometry. Problems that are of increasing importance to the transport community are those that contain subdomains which are considered optically thick and diffusive. These problems result in high computational costs and grid refinement that make realistic models impossible to solve. As a result, we look to develop vertex-based characteristic methods that can reproduce these diffusive solutions with spatial grids that do not resolve boundary layers. This research will allow for continued development of advanced conservative characteristic methods with better properties for R-Z geometries.

The transport methods derived here are based on a change of coordinates that removes the angular derivative term in the differential operator resulting in a differential equation which can be discretized using methods similar to those found in 1-D slab geometry. In this study, we present a family of characteristic methods; Vladimirov's method of characteristics, a conservative long characteristic method, two locally conservative short characteristic methods, a linear long characteristic method, and an explicit slope long characteristic method. The numerical results presented in this thesis demonstrate the performance of each method, and the asymptotic diffusion limit analysis shows a method's behavior for diffusive

problems. We found that the linear and explicit slope long characteristic methods generated numerical solutions which are well behaved in diffusive problems. Also, we analyzed several of these methods using asymptotic diffusion limit analysis and found that the linear long characteristic method limits to a discretized version of the diffusion equation.

Characteristic Methods for Solving the Particle Transport Equation in 1-D
Spherical Geometry

by
John T. Fleming III

A thesis submitted to the Graduate Faculty of
North Carolina State University
in partial fulfillment of the
requirements for the Degree of
Master of Science

Nuclear Engineering

Raleigh, North Carolina

2009

APPROVED BY:

_____   _____
Dr. Zhilin Li   Dr. Yousry Y. Azmy

_____   _____
Dr. Dmitriy Y. Anistratov   Dr. Paul J. Turinsky
Chair of Advisory Committee

DEDICATION

To Harmony, Skylar, and Koen. Thank you for your love and support.

"Making no mistakes is what establishes the certainty of victory, for it means conquering

an enemy that is already defeated." - Sun Tzu

BIOGRAPHY

John Thomas Fleming III was born in East Moline, Illinois on December 21, 1975. He graduated from Saint Xavier High School in Louisville, KY in 1994 and shortly after joined the United States Navy where he served as a Nuclear Reactor Operator aboard the submarine USS Columbia.

After six years of service, John continued his education by graduating from Whatcom Community College and later completed his bachelors degree in Nuclear Engineering from Oregon State University. He then entered graduate school at North Carolina State University to continue his studies in the field of nuclear engineering.

John is married to Harmony Fleming, and they have one child Skylar and are expecting a second, Koen. John and Harmony are looking to relocate to the west coast where they intend to settle their family and pursue careers related to their fields of study.

ACKNOWLEDGEMENTS

TABLE OF CONTENTS

LIST OF FIGURES

LIST OF TABLES

Chapter 1

INTRODUCTION

1.1 Overview

Many science and engineering applications utilize processes described by the particle transport (linear Boltzmann) equation, such as radiation shielding, reactor physics, and astrophysics calculations. These applications analyze realistic phenomena that have a degree of variability and require modeling of complex geometries such that analytic methods fail to provide solutions to current problems. Properly simulating these processes has provided the motivation to develop numerical techniques that can efficiently solve particle transport problems. Some radiative transport problems have material properties and mesh sizes that are considered "optically thin", methods designed for these problem types address solution behaviors that can be analyzed using truncation error analysis; i.e. as the size of a cell tends towards zero. This study, however, will address problems that are considered "optically thick" and diffusive.

Diffusive problems have been a constant focus of computational physicists for several decades, with the intent of developing numerical methods that, accurately and efficiently, represent the interaction of radiation with matter in sophisticated multiphysics models. These systems typically contain regions that have a large number of interactions per unit path length with few particles removed due to these interactions. Problems of this type result in high computation costs when using standard approaches, due to the grid refinement necessary to generate an acceptable solution. Therefore, current research utilizes diffusion limit analysis to determine the behavior of a method for problems where the spatial cells are considered optically thick and diffusive. This thesis looks at the development and analysis of methods for 1-D spherical geometry which will produce accurate solutions in diffusive regions.

1.2   The Boltzmann Transport Equation

This work begins with a description of the linear Boltzmann equation. The Boltzmann equation has been studied for over a century. Originally formulated to describe the dynamics of an ideal gas, it was later applied to the study of radiation transfer in astrophysics problems and particle transport within nuclear reactors. The increasing sophistication of model problems and advent of computer technology eventually shifted research from analytic techniques to more numerical based methods.

The transport equation in its most general form is a function of seven independent variables: 3 spatial, 2 angular, time, and energy. This thesis considers the steady-state,

one-group particle transport equation with isotropic-scattering

$$\vec{\Omega} \cdot \vec{\nabla}\psi(\vec{r},\vec{\Omega}) + \sigma_t(\vec{r})\psi(\vec{r},\vec{\Omega}) = \frac{1}{4\pi}\sigma_s(\vec{r})\int_{4\pi}\psi(\vec{r},\vec{\Omega}')d\vec{\Omega}' + \frac{1}{4\pi}q(\vec{r}),\qquad (1.1)$$

$$\vec{r} \in \Gamma,\ \vec{r}_b \in \partial\Gamma\,,\qquad (1.2)$$

$$\psi(\vec{r},\vec{\Omega})|_{\vec{r}\in\partial\Gamma} = \psi^{in}(\vec{r}_b,\vec{\Omega}),\ \vec{\Omega}\cdot\vec{n} < 0,\qquad (1.3)$$

where $\psi[\frac{\#of particles}{sec\cdot cm^2}]$ is the angular flux, $\sigma_t[cm^{-1}]$ is the total cross section, $\sigma_s[cm^{-1}]$ is the scattering cross section, and $q[\frac{\#of particles}{sec\cdot cm^3}]$ represents the external source.

These are realistic simplification. First, energy dependent problems can be looked at as a series of coupled energy independent problems, where each energy group is coupled though the scattering term on the right hand side (RHS) of the transport equation. Second, time dependence adds a level of complexity which requires discretization techniques that are independent of the spatial and angular methods presented.

1.2.1 Curvilinear Geometries

In more compact form, Eq. (1.1) can be written in terms of linear operators

$$L\psi = S\psi + Q\,,\qquad (1.4)$$

$$L\psi = \vec{\Omega}\cdot\vec{\nabla}\psi(\vec{r},\vec{\Omega}) + \sigma_t(\vec{r})\psi(\vec{r},\vec{\Omega})\,,\qquad (1.5)$$

$$S\psi = \frac{1}{4\pi}\sigma_s(\vec{r})\int_{4\pi}\psi(\vec{r},\vec{\Omega}')d\vec{\Omega}'\,,\qquad (1.6)$$

where L is the streaming and removal operator, S is the scattering operator, and Q is the external source. For the purpose of explaining different geometries, L is the operator of interest, specifically, the streaming term, $\vec{\Omega}\cdot\vec{\nabla}\psi$. In this study, the 1-D spherical geometry

3

is considered. In these problems, we express the particle direction of motion with respect to its radius vector, $\vec{r}$ such that

$$\mu = \vec{\Omega} \cdot \hat{r} = \cos\theta \,, \ \hat{r} = \frac{\vec{r}}{|\vec{r}|} \,. \tag{1.7}$$

Now, one can see from Eq. (1.7) that as a particle travels along direction $\vec{\Omega}$ the value of the direction cosine, μ, will continue to change, which results in an angular derivative term in the streaming operator

$$\frac{d\psi}{ds} = \frac{\partial\psi}{\partial r}\frac{dr}{ds} + \frac{\partial\psi}{\partial\mu}\frac{d\mu}{ds}, \tag{1.8}$$

where

$$\frac{dr}{ds} = \cos\theta = \mu, \tag{1.9}$$

$$\frac{d\mu}{ds} = \frac{d\cos\theta}{d\theta}\frac{d\theta}{ds} = \sin\theta\frac{\sin\theta}{r}\,, \tag{1.10}$$

$$\frac{d\mu}{ds} = \frac{(1-\mu^2)}{r}\,. \tag{1.11}$$

Substituting Eq. (1.9) and Eq. (1.11) into Eq. (1.8) yields the following streaming operator

$$\frac{d\psi}{ds} = \mu\frac{\partial\psi}{\partial r} + \frac{(1-\mu^2)}{r}\frac{\partial\psi}{\partial\mu}\,, \tag{1.12}$$

and substituting Eq. (1.12) into Eq. (1.1) gives the 1-D, one-group, steady-state, spherical geometry transport equation

$$\mu\frac{\partial\psi}{\partial r} + \frac{(1-\mu^2)}{r}\frac{\partial\psi}{\partial\mu} + \sigma_t(r)\psi(r,\mu) = \frac{1}{2}\sigma_s(r)\int_{-1}^{1}\psi(r,\mu')d\mu' + \frac{1}{2}q(r)\,, \tag{1.13}$$

$$0 \leq r \leq R, \ -1 \leq \mu \leq 1\,, \tag{1.14}$$

$$\psi(R,\mu) = \psi^{in}(\mu), \ \mu < 0\,. \tag{1.15}$$

Note that the equation (1.13) can be written in the following divergence form:

$$\frac{1}{r^2}\frac{\partial}{\partial r}(r^2\mu\psi) + \frac{\partial}{\partial\mu}\left(\frac{1-\mu^2}{r}\psi\right) + \sigma_t(r)\psi(r,\mu) = \frac{1}{2}\sigma_s(r)\int_{-1}^{1}\psi(r,\mu')d\mu' + \frac{1}{2}q(r)\,. \tag{1.16}$$

1.3 Asymptotic Diffusion Analysis

The linear Boltzmann equation can behave differently based on the physical conditions of a system. Because transport problems can posses multiple regions with varying material properties, it is important to understand how the transport equation behaves for a given set of parameters. One such behavior, which has importance in many radiative transfer applications, is how the transport equation limits to the diffusion equation as the system becomes large compared to a particle's mean free path (optically thick) with very little absorption and source. The asymptotic diffusion limit analysis is presented here for the continuous case, and is also used later as a tool that will help to determine accuracy of a numerical method [11, 16]. The analysis is presented for the 1-D spherical geometry case with isotropic scattering

$$\mu \frac{\partial \psi}{\partial r} + \frac{(1 - \mu^2)}{r} \frac{\partial \psi}{\partial \mu} + \sigma_t(r)\psi(r, \mu) = \frac{1}{2}\sigma_s(r) \int_{-1}^{1} \psi(r, \mu')d\mu' + \frac{1}{2}q(r), \tag{1.17}$$

$$0 \leq r \leq R, \; -1 \leq \mu \leq 1, \tag{1.18}$$

$$\psi(R, \mu) = \psi^{in}(\mu), \; \mu < 0. \tag{1.19}$$

Now, a dimensionless parameter, ε, is introduced such that as $\varepsilon \to 0$ the system becomes more optically thick while the source and absorption cross section are reduced.

$$\sigma_t(r) = \frac{\hat{\sigma}_t(r)}{\varepsilon}, \tag{1.20}$$

$$\sigma_a(r) = \varepsilon\hat{\sigma}_a(r), \tag{1.21}$$

$$q(r) = \varepsilon\hat{q}(r), \tag{1.22}$$

where $\hat{\sigma}_t(r)$, $\hat{\sigma}_s(r)$, $\hat{q}(r)$ are O(1). Substituting Eq. (1.20), (1.21), (1.22) into Eq.(1.17) yields the following scaled transport equation

$$\mu \frac{\partial \psi}{\partial r} + \frac{(1-\mu^2)}{r}\frac{\partial \psi}{\partial \mu} + \frac{\hat{\sigma}_t(r)}{\varepsilon}\psi(r,\mu) = \frac{1}{2}\left[\frac{\hat{\sigma}_t(r)}{\varepsilon} - \varepsilon\hat{\sigma}_a(r)\right]\int_{-1}^{1}\psi(r,\mu')d\mu' + \frac{1}{2}\varepsilon\hat{q}(r). \quad (1.23)$$

Now we introduce the ansatz

$$\psi(r,\mu) = \sum_{m=0}^{\infty}\psi^{(m)}(r,\mu)\varepsilon^m\,, \quad (1.24)$$

substitute the expansion (1.24) into Eq. (1.23) and equate coefficients for different powers of ε. The following results are obtained for ε^0, ε^1, ε^2 respectively

$$\psi^{(0)}(r,\mu) = \frac{1}{2}\phi^{(0)}(r)\,, \quad (1.25)$$

$$\psi^{(1)}(r,\mu) = \frac{1}{2}\phi^{(1)}(r) - \frac{\mu}{2\hat{\sigma}_t(r)}\frac{d\phi^{(0)}}{dr}(r)\,, \quad (1.26)$$

$$\hat{\sigma}_t(r)\left[\psi^{(2)}(r,\mu) - \frac{1}{2}\phi^{(2)}(r)\right] = -\frac{\mu}{2}\frac{d\phi^{(1)}}{dr}(r) + \frac{\mu^2}{2}\frac{d}{dr}\frac{1}{\hat{\sigma}_t(r)}\frac{d\phi^{(0)}}{dr}(r) +$$

$$\frac{1}{2r\hat{\sigma}_t(r)}\frac{d\phi^{(0)}}{dr}(r) - \frac{\mu^2}{2r\hat{\sigma}_t(r)}\frac{d\phi^{(0)}}{dr}(r) - \frac{\hat{\sigma}_a}{2}\phi^{(0)}(r) + \frac{1}{2}\hat{q}(r)\,, \quad (1.27)$$

where

$$\phi^{(m)}(r) = \int_{-1}^{1}\psi^{(m)}(r,\mu')d\mu'\,. \quad (1.28)$$

Integrating Eq. (1.27) over all values of μ results in the following solvability condition

$$-\frac{1}{r^2}\frac{d}{dr}\left(\frac{r^2}{3\hat{\sigma}_t(r)}\frac{d\phi^{(0)}(r)}{dr}\right) + \hat{\sigma}_a(r)\phi^{(0)}(r) = \hat{q}(r)\,. \quad (1.29)$$

If this condition is not satisfied then no solution of Eq. (1.27) exists. Now, we multiply Eq. (1.29) by ε and use Eq. (1.20), (1.21), and (1.22) to obtain the diffusion equation for $\phi^{(0)}$

$$-\frac{1}{r^2}\frac{d}{dr}\left(\frac{r^2}{3\sigma_t(r)}\frac{d\phi^{(0)}(r)}{dr}\right) + \sigma_a(r)\phi^{(0)}(r) = q(r)\,. \quad (1.30)$$

6

This analysis shows that the leading order angular flux is isotropic and satisfies the conventional diffusion equation for the interior of the diffusive region with boundary condition

$$\phi^{(0)}(R) = 2 \int_{-1}^{1} W(|\mu|)\psi^{in}(\mu)d\mu.$$ (1.31)

Here, $W(\mu)$, related to the Chandrasekhar's X function [4], satisfies

$$W(\mu) = 0.956\mu + 1.565\mu^2 \pm .0035 \approx \mu + \frac{3}{2}\mu^2.$$ (1.32)

1.4 Brief History

There have been many notable advancements in the development of numerical techniques for curvilinear geometries, specificly 1-D spherical geometries. There are two main groups of methods that have been considered, discrete ordinate methods, which rely on an independent discretization of the angular and spatial variables, and characteristic methods, which solve the transport equation along a characteristic path, aligned in a particular direction. The later consists of two types, short and long characteristics. Short characteristics are path lengths that span the length of an individual cell where long characteristics span the entire spatial grid.

Most method development in 1-D spherical geometry have been in discrete ordinates. Its simplicity in Cartesian geometries is lost in curvilinear geometries due to the angular derivative term in the steaming operator of the transport equation. Now, adequate differencing techniques must be derived for both the angular and spatial variables. One of the existing angular differencing techniques is Weighted Diamond Differencing (WDD). Morel and Montry [12] found that, combined with starting direction flux values, WDD

produces accurate solutions in diffusive type problems given the appropriate spatial discretization. Later, several angular differencing approximations were analyzed in [19]. The P_{N-1}-Equivalent S_n angular discretization was proposed in [21]. Note that the P_N approximation yields accurate results for optically thick diffusive problems [13]. A notable advancement in spatial discretization for 1-D spherical geometry was the asymptotic analysis of "simple" corner balance and "fully-lumped" discontinuous finite element methods [17]. Both were found to be accurate in the thick diffusion limit.

Vladimirov [2, 3] proposed methods of long characteristics (VMOC) for 1-D spherical geometry. He posed a set of vertex-based methods that utilized a characteristic form of the 1-D spherical geometry transport equation. He treated the total source term with either linear or parabolic interpolation. These are not conservative. The idea of a conservative version of VMOC was proposed in [14]. The method of characteristic tubes [8] expand on VMOC by solving the transport equation along a volume average characteristic or a "characteristic tube". Here, each tube is defined by the volume between the characteristics. This produced a method that retained the favorable qualities of VMOC but also preserved the particle balance in a cell resulting in increased solution accuracy. Askew [10] also considered a version of the method of tubes with step characteristics and applied it to general geometry. These techniques provide a basis for developing characteristic methods in 1-D spherical geometry and some have been shown to be accurate for non-diffusive problems. Recently, two moment-based versions of the method of tubes were developed [23], step and linear characteristics, and analyzed for accuracy in diffusive problems. The analysis found that step characteristics behaved poorly in diffusive regions, while linear characteristics did

meet the asymptotic diffusion limit.

1.5   Thesis Organization

The goal of this research is to develop a family of vertex-based characteristic methods for transport problems in 1-D spherical geometry that produce accurate solutions in the asymptotic diffusion limit. The transport methods derived here are based on transformation of the spherical geometry transport equation to a coordinate system based on the direction along characteristics and the perpendicular one, which results in the space where characteristics are straight lines. This transformation yields a first order differential equation that can be discretized using methods similar to those used in 1-D slab geometry.

Chapter 2 considers the first vertex-based characteristic discretization schemes developed by Vladimirov [2, 3]. Here we describe the transformation of the coordinate systems. Then we derive VMOC with linear and parabolic interpolation of the total source term and perform an asymptotic analysis of each method. These are non-conservative methods with no expectations of meeting the asymptotic diffusion limit. They did, however, provide a basis for developing the new characteristic methods described in this thesis.

In chapters 3 and 4, we derive the conservative versions of the methods of long and locally conservative short characteristics, linear long characteristic method, and the explicit slope long characteristic method and perform the asymptotic analysis for several of these methods. We have tested each of these methods using a set of problems which check solution behavior for both optically thin and diffusive problems. These numerical results are given in Chapter 5. We conclude with a discussion in Chapter 6.

The main results of the research were presented at the 2008 American Nuclear Society Annual Meeting and published in its transactions [22].

1.6   Acknowledgements

Chapter 2

VLADIMIROV'S METHOD OF

LONG CHARACTERISTICS

This chapter discusses characteristic methods developed for the treatment of spatially symmetric spheres and provides the basis for the family of methods presented in this thesis. The first of these methods was developed by V. Vladimirov [2, 3]. They utilize a coordinate system based on the characteristic track and its perpendicular direction. Transformation from the (r, μ) rectangular coordinates to this natural system removes the angular derivative in the differential operator term of Eq. (1.13) and reduces the spherical geometry transport equation to a first order differential equation, which can then be solved for a general solution along the characteristic path. This technique is used for the methods derived in the following sections.

2.1 Transformation of 1D Spherical Transport Equation to Local Orthogonal Coordinates

Consider the transport equation for 1D spherical geometry with isotropic scattering given by Eq. (1.13)

$$\mu \frac{\partial \psi}{\partial r} + \frac{(1 - \mu^2)}{r} \frac{\partial \psi}{\partial \mu} + \sigma_t(r)\psi(r, \mu) = \frac{1}{2}\sigma_s(r) \int_{-1}^{1} \psi(r, \mu')d\mu' + \frac{1}{2}q(r) , \tag{2.1}$$

$$0 \le r \le R, \ -1 \le \mu \le 1 ,$$

with an incident flux at $r = R$

$$\psi(R, \mu) = \psi^{in}(\mu) \text{ for } \mu < 0 . \tag{2.2}$$

Here $\psi(r, \mu)$ is the angular flux, σ_t and σ_s are the total and scattering cross sections, respectively, and q is an external source. Now, we begin the change of coordinates by defining the follow independent variables [1, 2, 3]

$$x = r\mu, \ \ y = r\sqrt{1 - \mu^2} , \tag{2.3}$$

$$-R \le x \le R, \ \ 0 \le y \le R .$$

Differentiate Eq. (2.3) with respect to r and μ

$$\frac{\partial x}{\partial r} = \mu , \ \ \frac{\partial x}{\partial \mu} = r , \ \ \frac{\partial y}{\partial r} = \sqrt{1 - \mu^2} , \ \ \frac{\partial y}{\partial \mu} = \frac{-r\mu}{\sqrt{1 - \mu^2}} . \tag{2.4}$$

From Eq. (2.3) and Eq. (2.4) we can define the following

$$\frac{\partial \psi}{\partial r} = \frac{\partial \psi}{\partial x}\frac{dx}{dr} + \frac{\partial \psi}{\partial y}\frac{dy}{dr} = \mu \frac{\partial \psi}{\partial x} + \sqrt{1 - \mu^2}\frac{\partial \psi}{\partial y} , \tag{2.5}$$

$$\frac{\partial \psi}{\partial \mu} = \frac{\partial \psi}{\partial x}\frac{dx}{d\mu} + \frac{\partial \psi}{\partial y}\frac{dy}{d\mu} = r \frac{\partial \psi}{\partial x} + \frac{-r\mu}{\sqrt{1 - \mu^2}}\frac{\partial \psi}{\partial y} . \tag{2.6}$$

Substituting Eq. (2.5) and Eq. (2.6) into the first two terms on the left hand side (LHS) of Eq. (2.1) yields the following streaming operator

$$\mu\left(\mu\frac{\partial\psi}{\partial x}+\sqrt{1-\mu^2})\frac{\partial\psi}{\partial y}\right)+\frac{(1-\mu^2)}{r}\left(r\frac{\partial\psi}{\partial x}+\frac{-r\mu}{\sqrt{1-\mu^2}}\frac{\partial\psi}{\partial y}\right)=\frac{\partial\psi(x,y)}{\partial x}. \qquad (2.7)$$

The final result is the 1D spherical geometry transport equation in local orthogonal coordinate system

$$\frac{\partial\psi(x,y)}{\partial x}+\sigma_t(\sqrt{x^2+y^2})\psi(x,y)=\frac{1}{2}\sigma_s(\sqrt{x^2+y^2})\phi(\sqrt{x^2+y^2})+\frac{1}{2}q(\sqrt{x^2+y^2}), \qquad (2.8)$$

with an incident flux at $r = R$

$$\psi(-\sqrt{R^2-y^2},y)=\psi^{in}(y), \quad 0\le y\le R. \qquad (2.9)$$

We now solve the first order differential equation for a general solution between x_o and x for a given y

$$\psi(x,y)=\psi(x_o,y)e^{-\int_{x_o}^x \sigma_t dx''}+\int_{x_o}^x Q(\sqrt{x^2+y^2})e^{-\int_{x'}^x \sigma_t dx''}dx', \qquad (2.10)$$

where

$$Q(\sqrt{x^2+y^2})=\frac{1}{2}\sigma_s(\sqrt{x^2+y^2})\phi(\sqrt{x^2+y^2})+\frac{1}{2}q(\sqrt{x^2+y^2}). \qquad (2.11)$$

2.2   Vladimirov's Method of Long Characteristics(VMOC)

Now, we can generate the spatial grid used by VMOC shown in Figure. 2.2 by dividing r into N intervals $[r_{k+1/2}, r_{k-1/2}]$ and forcing $y_{i-1/2} = r_{i-1/2}$. The resulting spatial grid in (x, y) variables is given by
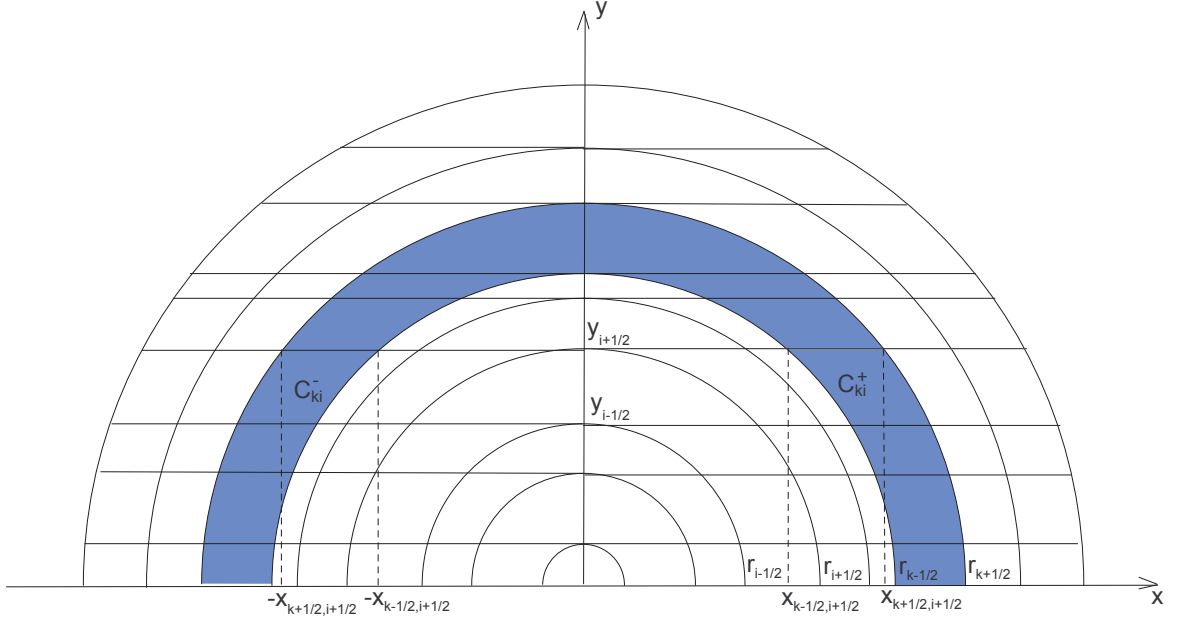
Figure 2.1: The characteristics in (x, y) coordinates.

$$(\pm x_{k-1/2,i-1/2}, y_{i-1/2}),\ k = i, .., N+1,\ \ i = 1, .., N+1\,, \tag{2.12}$$

$$x_{k-1/2,i-1/2} = \sqrt{r_{k-1/2}^2 - r_{i-1/2}^2},\ \ y_{i-1/2} = r_{i-1/2}\,. \tag{2.13}$$

Using Eq. (2.3) and Eq. (2.12), we can define the spatially dependent angular mesh

$$\mu_{k-1/2,i-1/2} = \sqrt{1 - \frac{r_{i-1/2}^2}{r_{k-1/2}^2}}\,. \tag{2.14}$$

Evaluating Eq. (2.10) at $x = -x_{k-1/2,i-1/2}$, $x_o = -x_{k+1/2,i-1/2}$, and $y_{i-1/2}$ yields

$$\begin{aligned}
\psi_{k-1/2,i-1/2}^- = \psi_{k+1/2,i-1/2}^- e^{-\sigma_{t,k}\Delta x_{k,i-1/2}} \\
+ \int_{-x_{k+1/2,i-1/2}}^{-x_{k-1/2,i-1/2}} Q(\sqrt{x^2 + y_{i-1/2}^2}) e^{\sigma_{t,k}(x + x_{k-1/2,i-1/2})} dx\,,
\end{aligned} \tag{2.15}$$

$$\psi_{N+1/2,i-1/2}^- = \psi^{in}(y_{i-1/2})\,, \tag{2.16}$$

$$k = N+1, ..., i\,. $$

14

Evaluating Eq. (2.10) at $x = x_{k+1/2,i-1/2}$, $x_o = x_{k-1/2,i-1/2}$, and $y_{i-1/2}$ yields

$$
\begin{aligned}
\psi^+_{k+1/2,i-1/2} = &\ \psi^+_{k-1/2,i-1/2} e^{-\sigma_{t,k}\Delta x_{k,i-1/2}} \\
&+ \int_{x_{k-1/2,i-1/2}}^{x_{k+1/2,i-1/2}} Q(\sqrt{x^2 + y^2_{i-1/2}}) e^{-\sigma_{t,k}(x_{k+1/2,i-1/2}-x)} dx \,,
\end{aligned}
\tag{2.17}
$$

$$
\psi^+_{i-1/2,i-1/2} = \psi^-_{i-1/2,i-1/2} \,,
\tag{2.18}
$$

$$
k = i, .., N+1 \,,
$$

$$
\text{for} \quad i = 1, ..., N+1 \,.
$$

Here

$$
\psi^-_{k-1/2,i-1/2} = \psi(-x_{k-1/2,i-1/2}, y_{i-1/2}) \,,
\tag{2.19}
$$

$$
\psi^+_{k-1/2,i-1/2} = \psi(x_{k-1/2,i-1/2}, y_{i-1/2}) \,,
\tag{2.20}
$$

$$
Q(\sqrt{x^2+y^2}) = \frac{1}{2}\left(\sigma_s(\sqrt{x^2+y^2})\phi(\sqrt{x^2+y^2}) + q(\sqrt{x^2+y^2})\right) \,,
\tag{2.21}
$$

$$
\Delta x_{k,i-1/2} = x_{k+1/2,i-1/2} - x_{k-1/2,i-1/2} \,.
\tag{2.22}
$$

The integrals in Eqs. (2.15) and (2.17) are approximated in the following way:

$$
\begin{aligned}
&\int_{-x_{k+1/2,i-1/2}}^{-x_{k-1/2,i-1/2}} Q(\sqrt{x^2+y^2_{i-1/2}}) e^{\sigma_{t,k}(x+x_{k-1/2,i-1/2})} dx \\
&= G^-_{k,i-1/2} Q_{k-1/2,i-1/2} + P^-_{k,i-1/2} Q_{k+1/2,i-1/2} \,,
\end{aligned}
\tag{2.23}
$$

$$
\begin{aligned}
&\int_{x_{k-1/2,i-1/2}}^{x_{k+1/2,i-1/2}} Q(\sqrt{x^2+y^2_{i-1/2}}) e^{-\sigma_{t,k}(x_{k+1/2,i-1/2}-x)} dx \\
&= P^+_{k,i-1/2} Q_{k-1/2,i-1/2} + G^+_{k,i-1/2} Q_{k+1/2,i-1/2} \,,
\end{aligned}
\tag{2.24}
$$

where

$$
Q_{k-1/2,i-1/2} = Q(\sqrt{x^2_{k-1/2} + y^2_{i-1/2}}) \,.
$$

The first condition to determine the coefficients $P_{k,i-1/2}^{\pm}$ and $G_{k,i-1/2}^{\pm}$ requires that Eqs. (2.23) and Eqs. (2.24) are exact, if

$$Q_{k-1/2,i-1/2} = Q_{k+1/2,i-1/2} = 1 \,. \tag{2.25}$$

This leads to

$$G_{k,i-1/2}^{\pm} = \frac{1}{\sigma_{t,k}}(1 - e^{-\sigma_{t,k}\Delta x_{k,i-1/2}}) - P_{k,i-1/2}^{\pm} \,. \tag{2.26}$$

In this case, Eqs. (2.15) and (2.17) give rise to

$$\psi_{k-1/2,i-1/2}^{-} = \psi_{k+1/2,i-1/2}^{-}e^{-\tau_{k,i-1/2}} + P_{k,i-1/2}^{-}Q_{k+1/2,i-1/2}$$
$$+ \left[\frac{1}{\sigma_{t,k}}(1 - e^{-\tau_{k,i-1/2}}) - P_{k,i-1/2}^{-}\right]Q_{k-1/2,i-1/2} \,, \tag{2.27}$$

$$\psi_{k+1/2,i-1/2}^{+} = \psi_{k-1/2,i-1/2}^{+}e^{-\tau_{k,i-1/2}} + P_{k,i-1/2}^{+}Q_{k-1/2,i-1/2}$$
$$+ \left[\frac{1}{\sigma_{t,k}}(1 - e^{-\tau_{k,i-1/2}}) - P_{k,i-1/2}^{+}\right]Q_{k+1/2,i-1/2} \,, \tag{2.28}$$

where

$$\tau_{k,i-1/2} = \sigma_{t,k}\Delta x_{k,i-1/2} \,.$$

Additional conditions are needed to determine the $P_{k,i-1/2}^{\pm}$ coefficients. Now, we consider two variations for treating the total source in a cell, linear and parabolic interpolation.

2.2.1 VMOC with Linear Interpolation of the Total Source Term

To derive the method with linear interpolation of the total source with respect to x, we impose the condition that Eq. (2.23) is exact for $Q = x$, then Eq. (2.23) becomes

$$\int_{-x_{k+1/2,i-1/2}}^{-x_{k-1/2,i-1/2}} xe^{\sigma_{t,k}(x+x_{k-1/2,i-1/2})}dx =$$

$$x_{k+1/2,i-1/2}P_{k,i-1/2}^{-} + x_{k-1/2,i-1/2}\left[\frac{1}{\sigma_{t,k}}(1 - e^{-\tau_{k,i-1/2}}) - P_{k,i-1/2}^{-}\right] \,, \tag{2.29}$$

16

and performing the integration

$$
\int_{-x_{k+1/2,i-1/2}}^{-x_{k-1/2,i-1/2}} x e^{\sigma_{t,k}(x+x_{k-1/2,i-1/2})} dx =
$$

$$
-\frac{1}{\sigma_{t,k}} \left(x_{k+1/2,i-1/2}\, e^{-\tau_{k,i-1/2}} - x_{k-1/2,i-1/2} + \frac{1}{\sigma_{t,k}}(e^{-\tau_{k,i-1/2}} - 1) \right). \tag{2.30}
$$

Equating the RHS of Eq. (2.29) to the RHS of Eq. (2.30), and solving for $P_{k,i-1/2}^-$ yields

$$
P_{k,i-1/2}^- = \frac{1}{\sigma_{t,k}} \left(\frac{1 - e^{-\tau_{k,i-1/2}}}{\tau_{k,i-1/2}} - e^{-\tau_{k,i-1/2}} \right). \tag{2.31}
$$

Next, we impose a similar condition that Eq. (2.24) is exact for $Q = x$, then Eq. (2.24)

becomes

$$
\int_{x_{k-1/2,i-1/2}}^{x_{k+1/2,i-1/2}} x e^{-\sigma_{t,k}(x_{k+1/2,i-1/2}-x)} dx =
$$

$$
x_{k-1/2,i-1/2} P_{k,i-1/2}^+ + x_{k+1/2,i-1/2} \left[\frac{1}{\sigma_{t,k}}(1 - e^{-\tau_{k,i-1/2}}) - P_{k,i-1/2}^+ \right], \tag{2.32}
$$

and performing the integration

$$
\int_{x_{k-1/2,i-1/2}}^{x_{k+1/2,i-1/2}} x e^{-\sigma_{t,k}(x_{k+1/2,i-1/2}-x)} dx =
$$

$$
-\frac{1}{\sigma_{t,k}} \left(x_{k+1/2,i-1/2}\, e^{-\tau_{k,i-1/2}} - x_{k-1/2,i-1/2} + \frac{1}{\sigma_{t,k}}(e^{-\tau_{k,i-1/2}} - 1) \right). \tag{2.33}
$$

Equating the RHS of Eq. (2.32) to the RHS of Eq. (2.33), and solving for $P_{k,i-1/2}^+$ yields

$$
P_{k,i-1/2}^+ = \frac{1}{\sigma_{t,k}} \left(\frac{1 - e^{-\tau_{k,i-1/2}}}{\tau_{k,i-1/2}} - e^{-\tau_{k,i-1/2}} \right), \tag{2.34}
$$

and as a result we find that

$$
P_{k,i-1/2}^+ = P_{k,i-1/2}^-. \tag{2.35}
$$

Hereafter the method defined by Eqs. (2.27), (2.28), (2.31), and (2.35) is referred to as

VMOC with linear interpolation of the total source (VMOC-LI).

2.2.2 VMOC with Parabolic Interpolation of the Total Source Term

To formulate the method with parabolic interpolation of the total source with respect to x, we require that Eq. (2.23) is exact for $Q = x^2$ and get

$$
\int_{-x_{k+1/2,i-1/2}}^{-x_{k-1/2,i-1/2}} x^2 e^{\sigma_{t,k}(x+x_{k-1/2,i-1/2})} dx =
$$

$$
x_{k+1/2,i-1/2}^2 P_{k,i-1/2}^- + x_{k-1/2,i-1/2}^2 \left[\frac{1}{\sigma_{t,k}}(1 - e^{-\tau_{k,i-1/2}}) - P_{k,i-1/2}^- \right], \tag{2.36}
$$

and performing the integration gives

$$
\int_{-x_{k+1/2,i-1/2}}^{-x_{k-1/2,i-1/2}} x^2 e^{\sigma_{t,k}(x+x_{k-1/2,i-1/2})} dx =
$$

$$
-\frac{1}{\sigma_{t,k}} \left(x_{k+1/2,i-1/2}^2 \, e^{-\tau_{k,i-1/2}} - x_{k-1/2,i-1/2}^2 + \frac{1}{\sigma_{t,k}}(e^{-\tau_{k,i-1/2}} - 1) \right). \tag{2.37}
$$

Now, equating the RHS of Eq. (2.36) to the RHS of Eq. (2.37), and solving for $P_{k,i-1/2}^-$

yields

$$
P_{k,i-1/2}^- = \frac{1}{\sigma_{t,k}} \left[\frac{2(\sigma_{t,k} x_{k+1/2,i-1/2} - 1)(1 - e^{-\tau_{k,i-1/2}})}{\sigma_{t,k}^2 (x_{k+1/2,i-1/2}^2 - x_{k-1/2,i-1/2}^2)} \right.
$$

$$
\left. + e^{-\tau_{k,i-1/2}} \left(\frac{2}{\sigma_{t,k}(x_{k+1/2,i-1/2} + x_{k-1/2,i-1/2})} - 1 \right) \right]. \tag{2.38}
$$

Next, we impose a similar condition that Eq. (2.24) is exact for $Q = x^2$, then Eq. (2.24)

becomes

$$
\int_{x_{k-1/2,i-1/2}}^{x_{k+1/2,i-1/2}} x^2 e^{-\sigma_{t,k}(x_{k+1/2,i-1/2}-x)} dx =
$$

$$
x_{k-1/2,i-1/2}^2 P_{k,i-1/2}^+ + x_{k+1/2,i-1/2}^2 \left[\frac{1}{\sigma_{t,k}}(1 - e^{-\tau_{k,i-1/2}}) - P_{k,i-1/2}^+ \right], \tag{2.39}
$$

and performing the integration gives

$$
\int_{x_{k-1/2,i-1/2}}^{x_{k+1/2,i-1/2}} x^2 e^{-\sigma_{t,k}(x_{k+1/2,i-1/2}-x)} dx =
$$

$$
-\frac{1}{\sigma_{t,k}} \left(x_{k+1/2,i-1/2}^2 \, e^{-\tau_{k,i-1/2}} - x_{k-1/2,i-1/2}^2 + \frac{1}{\sigma_{t,k}}(e^{-\tau_{k,i-1/2}} - 1) \right). \tag{2.40}
$$

Now, equating the RHS of Eq. (2.39) to the RHS of Eq. (2.40), and solving for $P^+_{k,i-1/2}$

yields

$$P^+_{k,i-1/2} = \frac{1}{\sigma_{t,k}} \left[\frac{2(\sigma_{t,k} x_{k+1/2,i-1/2} - 1)(1 - e^{-\tau_{k,i-1/2}})}{\sigma^2_{t,k}(x^2_{k+1/2,i-1/2} - x^2_{k-1/2,i-1/2})} \right.$$
$$\left. + e^{-\tau_{k,i-1/2}} \left(\frac{2}{\sigma_{t,k}(x_{k+1/2,i-1/2} + x_{k-1/2,i-1/2})} - 1 \right) \right]. \tag{2.41}$$

Hereafter the method defined by Eqs. (2.27), (2.28), (2.38), (2.41) is referred to as VMOC

with parabolic interpolation of the total source (VMOC-PI).

2.2.3 Quadratures

In both VMOC-LI and VMOC-PI, the scalar flux , $\phi(r)$ (at $r = r_{k-1/2}$), in the

scattering source term of Eq. (2.11) is calculated by means of integration of the cell-edge

angular flux, $\psi_{k-1/2,i-i/2}$, using the local angular mesh at $r = r_{k-1/2}$, namely, $\mu_{k-1/2,i-1/2}$,

$i = 1, ..., k$

$$\phi_{k-1/2} = \int_{-1}^{0} \psi^-_{k-1/2}(\mu) \, d\mu + \int_{0}^{1} \psi^+_{k-1/2}(\mu) \, d\mu, \tag{2.42}$$

$$\phi_{k-1/2} = \sum_{i=1}^{k} \int_{\mu_{k-1/2,i-1/2}}^{\mu_{k-1/2,i+1/2}} \psi^-_{k-1/2}(\mu) \, d\mu + \sum_{i=1}^{k} \int_{\mu_{k-1/2,i+1/2}}^{\mu_{k-1/2,i-1/2}} \psi^+_{k-1/2}(\mu) \, d\mu. \tag{2.43}$$

Using the trapezoid method, we get

$$\phi_{k-1/2} = \sum_{i=1}^{k} \psi^-_{k-1/2,i-1/2} w_{k-1/2,i-1/2} +$$
$$\sum_{i=1}^{k} \psi^+_{k-1/2,i-1/2} w_{k-1/2,i-1/2}, \tag{2.44}$$

where

$$w_{k-1/2,1/2} = \frac{1}{2}(\mu_{k-1/2,1/2} - \mu_{k-1/2,3/2}), \tag{2.45}$$

$$w_{k-1/2,i-1/2} = \frac{1}{2}(\mu_{k-1/2,i-3/2} - \mu_{k-1/2,i+1/2}), \ i = 2, ..., k-1,$$

$$w_{k-1/2,k-1/2} = \frac{1}{2}(\mu_{k-1/2,k-3/2} - \mu_{k-1/2,k-1/2}).$$

2.2.4 The Asymptotic Diffusion Analysis of VMOC

In this section, we perform an asymptotic diffusion analysis of the discretized equations of the VMOC methods to determine if they limit to a correct discretized version of the diffusion equation with appropriate boundary conditions. The analysis is similar to the continuous analysis as outlined in Section 1.3, except here the discrete equations are used. A detailed analysis is reproduced here, for VMOC-LI, with a summary of the major differences and final result for VMOC-PI.

Linear Interpolation

Consider Eqs. (2.27) and (2.28) in the following form:

$$
\psi^-_{k-1/2,i-1/2} - \psi^-_{k+1/2,i-1/2} + \sigma_{t,k}\Delta x_{k,i-1/2}\psi^-_{k,i-1/2} =
$$
$$
\frac{1}{2}(\sigma_{s,k}\Phi^-_{k,i-1/2} + q_k)\Delta x_{k,i-1/2}\,, \tag{2.46}
$$

$$
\psi^+_{k+1/2,i-1/2} - \psi^+_{k-1/2,i-1/2} + \sigma_{t,k}\Delta x_{k,i-1/2}\psi^+_{k,i-1/2} =
$$
$$
\frac{1}{2}(\sigma_{s,k}\Phi^+_{k,i-1/2} + q_k)\Delta x_{k,i-1/2}\,, \tag{2.47}
$$

where

$$
\psi^-_{k,i-1/2} = \alpha_{k,i-1/2}\psi^-_{k+1/2,i-1/2} + (1 - \alpha_{k,i-1/2})\psi^-_{k-1/2,i-1/2}\,, \tag{2.48}
$$

$$
\psi^+_{k,i-1/2} = \alpha_{k,i-1/2}\psi^-_{k-1/2,i-1/2} + (1 - \alpha_{k,i-1/2})\psi^-_{k+1/2,i-1/2}\,, \tag{2.49}
$$

$$
\Phi^-_{k,i-1/2} = \beta_{k,i-1/2}\phi_{k+1/2} + (1 - \beta_{k,i-1/2})\phi_{k-1/2}\,, \tag{2.50}
$$

$$
\Phi^+_{k,i-1/2} = \beta_{k,i-1/2}\phi_{k-1/2} + (1 - \beta_{k,i-1/2})\phi_{k+1/2}\,, \tag{2.51}
$$

$$
\alpha^\pm_{k,i-1/2} = \frac{1}{\tau_{k,i-1/2}} - \frac{e^{-\tau_{k,i-1/2}}}{(1 - e^{-\tau_{k,i-1/2}})}\,, \tag{2.52}
$$

and for linear interpolation

$$\beta^{\pm}_{k,i-1/2} = \frac{\sigma_{t,k}}{\left(1 - e^{-\tau_{k,i-1/2}}\right)} P^{\pm}_{k,i-1/2} = \alpha^{\pm}_{k,i-1/2} \, . \tag{2.53}$$

We define a small parameter ε, introduce scaled cross sections and source

$$\sigma_t = \frac{1}{\varepsilon}\hat{\sigma}_t \, , \quad \sigma_a = \varepsilon\hat{\sigma}_a \, , \quad q = \varepsilon\hat{q} \, , \tag{2.54}$$

and consider the transport problem as $\varepsilon \to 0$. Assume that the solution can be expanded

in power series of ε

$$\psi^{\pm}_{k-1/2,i-1/2} = \sum_{m=0}^{\infty} \varepsilon^m \psi^{\pm[m]}_{k-1/2,i-1/2} \, , \quad \psi^{\pm}_{k,i-1/2} = \sum_{m=0}^{\infty} \varepsilon^m \psi^{\pm[m]}_{k,i-1/2} \, , \quad \phi_k = \sum_{m=0}^{\infty} \varepsilon^m \phi^{[m]}_k \, .$$

$$\tag{2.55}$$

Note, if we introduce Eq. (2.54) into Eq. (2.52) and take the limit as $\varepsilon \to 0$, $\alpha^{\pm}_{k,i-1/2}$ can

be reduced to the following expression

$$\alpha^{\pm}_{k,i-1/2} = \lim_{\varepsilon \to 0} \left(\frac{\varepsilon}{\hat{\tau}_{k,i-1/2}} - \frac{e^{-\frac{\hat{\tau}_{k,i-1/2}}{\varepsilon}}}{1 - e^{-\frac{\hat{\tau}_{k,i-1/2}}{\varepsilon}}} \right) = \frac{\varepsilon}{\hat{\tau}_{k,i-1/2}} + o(\varepsilon^n) \quad \forall n \, , \tag{2.56}$$

where

$$\hat{\tau}_{k,i-1/2} = \hat{\sigma}_{t,k} \Delta x_{k,i-1/2} \, . \tag{2.57}$$

Now, we introduce the expansions (2.55) and weight (2.56) into Eqs. (2.46) - (2.51) and

equate the coefficients at powers of ε. This leads to the following sets of equations:

$O(\varepsilon^{-1})$ equations

$$\psi^{\pm[0]}_{k,i-1/2} = \frac{1}{2} \Phi^{\pm[0]}_{k,i-1/2} \, , \tag{2.58}$$

$O(1)$ equations

$$\psi^{-[0]}_{k-1/2,i-1/2} - \psi^{-[0]}_{k+1/2,i-1/2} + \hat{\tau}_{k,i-1/2}\left(\psi^{-[1]}_{k,i-1/2} - \frac{1}{2}\Phi^{-[1]}_{k,i-1/2}\right) = 0\,, \qquad (2.59)$$

$$\psi^{+[0]}_{k+1/2,i-1/2} - \psi^{+[0]}_{k-1/2,i-1/2} + \hat{\tau}_{k,i-1/2}\left(\psi^{+[1]}_{k,i-1/2} - \frac{1}{2}\Phi^{+[1]}_{k,i-1/2}\right) = 0\,, \qquad (2.60)$$

$$\psi^{-[0]}_{k,i-1/2} = \psi^{-[0]}_{k-1/2,i-1/2}\,, \qquad (2.61)$$

$$\psi^{+[0]}_{k,i-1/2} = \psi^{+[0]}_{k+1/2,i-1/2}\,, \qquad (2.62)$$

$$\Phi^{-[0]}_{k,i-1/2} = \phi^{[0]}_{k-1/2}\,, \qquad (2.63)$$

$$\Phi^{+[0]}_{k,i-1/2} = \phi^{[0]}_{k+1/2}\,, \qquad (2.64)$$

$O(\varepsilon)$ equations

$$\psi^{-[1]}_{k,i-1/2} = \frac{1}{\hat{\tau}_{k,i-1/2}}\left(\psi^{-[0]}_{k+1/2,i-1/2} - \psi^{-[0]}_{k-1/2,i-1/2}\right) + \psi^{-[1]}_{k-1/2,i-1/2}\,, \qquad (2.65)$$

$$\psi^{+[1]}_{k,i-1/2} = \frac{1}{\hat{\tau}_{k,i-1/2}}\left(\psi^{+[0]}_{k-1/2,i-1/2} - \psi^{+[0]}_{k+1/2,i-1/2}\right) + \psi^{+[1]}_{k-1/2,i-1/2}\,, \qquad (2.66)$$

$$\Phi^{-[1]}_{k,i-1/2} = \frac{1}{\hat{\tau}_{k,i-1/2}}\left(\phi^{[0]}_{k+1/2} - \phi^{[0]}_{k-1/2}\right) + \phi^{[1]}_{k-1/2}\,, \qquad (2.67)$$

$$\Phi^{+[1]}_{k,i-1/2} = \frac{1}{\hat{\tau}_{k,i-1/2}}\left(\phi^{[0]}_{k-1/2} - \phi^{[0]}_{k+1/2}\right) + \phi^{[1]}_{k+1/2}\,. \qquad (2.68)$$

Note that from Eq. (2.44) we have

$$\phi^{[m]}_{k-1/2} = \sum_{i=1}^{k}\psi^{-[m]}_{k-1/2,i-1/2}w_{k-1/2,i-1/2} + \sum_{i=1}^{k}\psi^{+[m]}_{k-1/2,i-1/2}w_{k-1/2,i-1/2}\,, \qquad (2.69)$$

and Eq. (2.18) gives

$$\psi^{+[m]}_{i-1/2,i-1/2} = \psi^{-[m]}_{i-1/2,i-1/2}\,. \qquad (2.70)$$

Using Eq. (2.70) and adjusting the weights accordingly, we can modify the definition of the scalar flux

$$\phi^{[m]}_{k-1/2} = \sum_{i=1}^{k}\psi^{-[m]}_{k-1/2,i-1/2}w^{-}_{k-1/2,i-1/2} + \sum_{i=1}^{k-1}\psi^{+[m]}_{k-1/2,i-1/2}w^{+}_{k-1/2,i-1/2}\,. \qquad (2.71)$$

where

$$w^{\pm}_{k-1/2,i-1/2} = w_{k-1/2,i-1/2}, \quad i = 1, ..., k-1, \tag{2.72}$$

$$w^{-}_{k-1/2,k-1/2} = 2w_{k-1/2,k-1/2},$$

$$w^{+}_{k-1/2,k-1/2} = 0.$$

First, we analyze the equations in the interior of the problem domain. The equations (2.59), evaluated at k, and (2.60), evaluated at $k-1$, are summed with weights $w^{\pm}_{k-1/2,i-1/2}$ over $1 \le i \le k$ and $1 \le i \le k-1$, respectively

$$\sum_{i=1}^{k} \frac{1}{\hat{\tau}_{k,i-1/2}} (\psi^{-[0]}_{k-1/2,i-1/2} - \psi^{-[0]}_{k+1/2,i-1/2}) w^{-}_{k-1/2,i-1/2} +$$
$$\sum_{i=1}^{k} (\psi^{-[1]}_{k,i-1/2} - \frac{1}{2}\Phi^{-[1]}_{k,i-1/2}) w^{-}_{k-1/2,i-1/2} = 0, \tag{2.73}$$

$$\sum_{i=1}^{k-1} \frac{1}{\hat{\tau}_{k-1,i-1/2}} (\psi^{+[0]}_{k-1/2,i-1/2} - \psi^{+[0]}_{k-3/2,i-1/2}) w^{+}_{k-1/2,i-1/2} +$$
$$\sum_{i=1}^{k-1} (\psi^{+[1]}_{k-1,i-1/2} - \frac{1}{2}\Phi^{+[1]}_{k-1,i-1/2}) w^{+}_{k-1/2,i-1/2} = 0. \tag{2.74}$$

Now, substitute Eqs. (2.65) and (2.67), evaluated at k, into Eq. (2.73), and substitute Eqs. (2.66) and (2.68), evaluated at $k-1$, into Eqs. (2.74)

$$\sum_{i=1}^{k} \psi^{-[1]}_{k-1/2,i-1/2} w^{-}_{k-1/2,i-1/2} - \frac{1}{2}\sum_{i=1}^{k} \frac{1}{\hat{\tau}_{k,i-1/2}} (\phi^{[0]}_{k+1/2} - \phi^{[0]}_{k-1/2}) w^{-}_{k-1/2,i-1/2}$$
$$- \frac{1}{2}\sum_{i=1}^{k} \phi^{[1]}_{k-1/2} w^{-}_{k-1/2,i-1/2} = 0, \tag{2.75}$$

$$\sum_{i=1}^{k-1} \psi^{+[1]}_{k-1/2,i-1/2} w^{+}_{k-1/2,i-1/2} - \frac{1}{2}\sum_{i=1}^{k-1} \frac{1}{\hat{\tau}_{k-1,i-1/2}} (\phi^{[0]}_{k-3/2} - \phi^{[0]}_{k-1/2}) w^{+}_{k-1/2,i-1/2}$$
$$- \frac{1}{2}\sum_{i=1}^{k-1} \phi^{[1]}_{k-1/2} w^{+}_{k-1/2,i-1/2} = 0. \tag{2.76}$$

23

Summing Eqs. (2.75) and (2.76) and introducing relationship (2.71) leads to the following approximation of the diffusion equation in interior cells

$$\left(\phi_{k+1/2}^{[0]} - \phi_{k-1/2}^{[0]}\right) \sum_{i=1}^{k} \frac{1}{\hat{\tau}_{k,i-1/2}} w_{k-1/2,i-1/2}^{-} -$$

$$\left(\phi_{k-1/2}^{[0]} - \phi_{k-3/2}^{[0]}\right) \sum_{i=1}^{k-1} \frac{1}{\hat{\tau}_{k-1,i-1/2}} w_{k-1/2,i-1/2}^{+} = 0 , \qquad (2.77)$$

$$k = 1, ..., N - 1 .$$

We notice that the VMOC-LI equations do not lead to an accurate discretization of the diffusion equation in the thick-diffusion limit.

We now consider the boundary cell to determine the asymptotic boundary condition. Equations (2.16), (2.58), (2.61), (2.63), and (2.69) give the Nth cell equation

$$\phi_{N+1/2}^{[0]} = \sum_{i=1}^{k} \psi^{in}(y_{i-1/2}) w_{N,i-1/2}^{-} + \frac{1}{2} \sum_{i=1}^{N-1} \phi_{N+1/2,i-1/2}^{[0]} w_{N,i-1/2}^{+} , \qquad (2.78)$$

and as a result, we have the asymptotic boundary condition of VMOC-LI defined as

$$\phi_{N+1/2}^{[0]} = \frac{\sum_{i=1}^{N} \psi^{in}(y_{i-1/2}) w_{N,i-1/2}^{-}}{\left(1 - \frac{1}{2} \sum_{i=1}^{N-1} w_{N,i-1/2}^{+}\right)} . \qquad (2.79)$$

Parabolic Interpolation

We now consider Vladimirov's method with parabolic interpolation of the total source. The VMOC-PI asymptotic analysis is the same as the analysis for VMOC-LI with the following changes to Eq. (2.53)

$$\beta_{k,i-1/2}^{-} = \frac{\sigma_{t,k}}{(1 - e^{-\tau_{k,i-1/2}})} P_{k,i-1/2}^{-} = \gamma_{1,k,i-1/2} + x_{k-1/2,i-1/2} \gamma_{2,k,i-1/2} , \qquad (2.80)$$

$$\beta_{k,i-1/2}^{+} = \frac{\sigma_{t,k}}{(1 - e^{-\tau_{k,i-1/2}})} P_{k,i-1/2}^{+} = \gamma_{1,k,i-1/2} + x_{k+1/2,i-1/2} \gamma_{2,k,i-1/2} , \qquad (2.81)$$

where

$$\gamma_{1,k,i-1/2} = \frac{2}{\sigma_{t,k}^2 (x_{k+1/2,i-1/2}^2 - x_{k-1/2,i-1/2}^2)} \,, \tag{2.82}$$

$$\gamma_{2,k,i-1/2} = \frac{2}{\sigma_{t,k}(x_{k+1/2,i}^2 - x_{k-1/2,i-1/2}^2)} \,. \tag{2.83}$$

Now, introducing the expansions (2.55) and weight (2.56) into Eqs. (2.46)-(2.51) and equating the coefficients at powers of ε, we note only two changes to the system of equations defined in the VMOC-LI analysis

$O(\varepsilon)$ equations

$$\Phi_{k,i-1/2}^{-[1]} = \hat{\gamma}_{2,k,i-1/2} x_{k-1/2,i-1/2} \left(\phi_{k+1/2}^{[0]} - \phi_{k-1/2}^{[0]} \right) + \phi_{k-1/2}^{[1]} \,, \tag{2.84}$$

$$\Phi_{k,i-1/2}^{+[1]} = \hat{\gamma}_{2,k,i-1/2} x_{k+1/2,i-1/2} \left(\phi_{k-1/2}^{[0]} - \phi_{k+1/2}^{[0]} \right) + \phi_{k+1/2}^{[1]} \,. \tag{2.85}$$

Following the same asymptotic diffusion analysis laid out by VMOC-LI, we derive the approximation of the diffusion equation in interior cells for VMOC-PI

$$\left(\phi_{k+1/2}^{[0]} - \phi_{k-1/2}^{[0]} \right) \sum_{i=1}^{k} \hat{\gamma}_{2,k,i-1/2} x_{k-1/2,i-1/2} w_{k-1/2,i-1/2} -$$

$$\left(\phi_{k-1/2}^{[0]} - \phi_{k-3/2}^{[0]} \right) \sum_{i=1}^{k-1} \hat{\gamma}_{2,k-1,i-1/2} x_{k-1/2,i-1/2} w_{k-1/2,i-1/2} = 0 \,,$$

$$\tag{2.86}$$

$$k = 1, ..., N - 1 \,.$$

The asymptotic boundary condition of VMOC-PI is defined in the same manner as VMOC-LI

$$\phi_{N+1/2}^{[0]} = \frac{\sum_{i=1}^{N} \psi^{in}(y_{i-1/2}) w_{N,i-1/2}}{\left(1 - \frac{1}{2} \sum_{i=1}^{N-1} w_{N,i-1/2}\right)} \,. \tag{2.87}$$

Both VMOC-LI and VMOC-PI methods yield discretized diffusion equations without absorption and source terms. This implies an unphysical approximation of the diffusive

equation. For example, using zero-flux boundary conditions would give a leading order solution of zero regardless of the value of the source term. As such, we say neither method limits to an accurate discretized diffusion equation. Furthermore, the boundary conditions derived in both VMOC-LI and VMOC-PI do not closely approximate those of the continuous form. These conclusions are confirmed in the numerical results chapter of this thesis.

Chapter 3

METHODS OF LONG

CHARACTERISTICS

In this chapter we consider a new family of vertex-based conservative long characteristic methods. The objective of this 1D work is to formulate methods which are accurate in the asymptotic thick diffusion limit and which will provide a necessary guidance for developing 2D characteristic methods for curvilinear geometries which are also well behaved.

3.1   Conservative Method of Long Characteristics

First, we formulate a conservative method of long characteristics in (x, y) variables that is based on an idea which was proposed in [14]. We start by integrating the transport equation along characteristics, as per section 2.1, approximate $Q(r)$ in each spatial cell with a cell-averaged value Q_k, and then evaluate Eq. (2.10) analytically for the kth cell.

Evaluating Eq.(2.10) at $x = -x_{k-1/2,i-1/2}$, $x_o = -x_{k+1/2,i-1/2}$, and $y_{i-1/2}$ yields

$$\psi_{k-1/2,i-1/2}^- = \psi_{k+1/2,i-1/2}^- e^{-\sigma_{t,k}\Delta x_{k,i-1/2}} + \frac{Q_k}{2\sigma_{t,k}}\left(1 - e^{-\tau_{k,i-1/2}}\right), \tag{3.1}$$

$$\psi_{N+1/2,i-1/2}^- = \psi^{in}(y_{i-1/2}), \tag{3.2}$$

$$k = N+1, ..., i. $$

Evaluating Eq. (2.10) at $x = x_{k+1/2,i-1/2}$, $x_o = x_{k-1/2,i-1/2}$, and $y_{i-1/2}$ yields

$$\psi_{k+1/2,i-1/2}^+ = \psi_{k-1/2,i-1/2}^+ e^{-\sigma_{t,k}\Delta x_{k,i-1/2}} + \frac{Q_k}{2\sigma_{t,k}}\left(1 - e^{-\tau_{k,i-1/2}}\right), \tag{3.3}$$

$$\psi_{i-1/2,i-1/2}^+ = \psi_{i-1/2,i-1/2}^-, \tag{3.4}$$

$$k = i, .., N+1, $$

$$\text{for} \quad i = 1, ..., N+1, $$

where

$$Q_k = \frac{1}{2}\left(\sigma_{s,k}\phi_k + q_k\right), \tag{3.5}$$

and ϕ_k and q_k are cell-average scalar flux and source

$$\phi_k = \frac{1}{v_k}\int_{r_{k-1/2}}^{r_{k+1/2}} \phi(r)r^2 dr, \tag{3.6}$$

$$v_k = \frac{r_{k+1/2}^3 - r_{k-1/2}^3}{3}. \tag{3.7}$$

We now derive the definition of ϕ_k that leads to a conservative method [14]. Let us consider a cell D_{ki}^+ in (r, μ) coordinates defined by lines $r = r_{k-1/2}$ and $r = r_{k+1/2}$ and characteristics (curves) $r\sqrt{1-\mu^2} = r_{i-1/2}$ and $r\sqrt{1-\mu^2} = r_{i+1/2}$ for $\mu > 0$ (see Figure 3.1). The balance in D_{ki}^+ is given by

$$\int_{D_{ki}^+} \left(L\psi(r,\mu) - Q(r)\right) r^2 dr d\mu = 0, \tag{3.8}$$
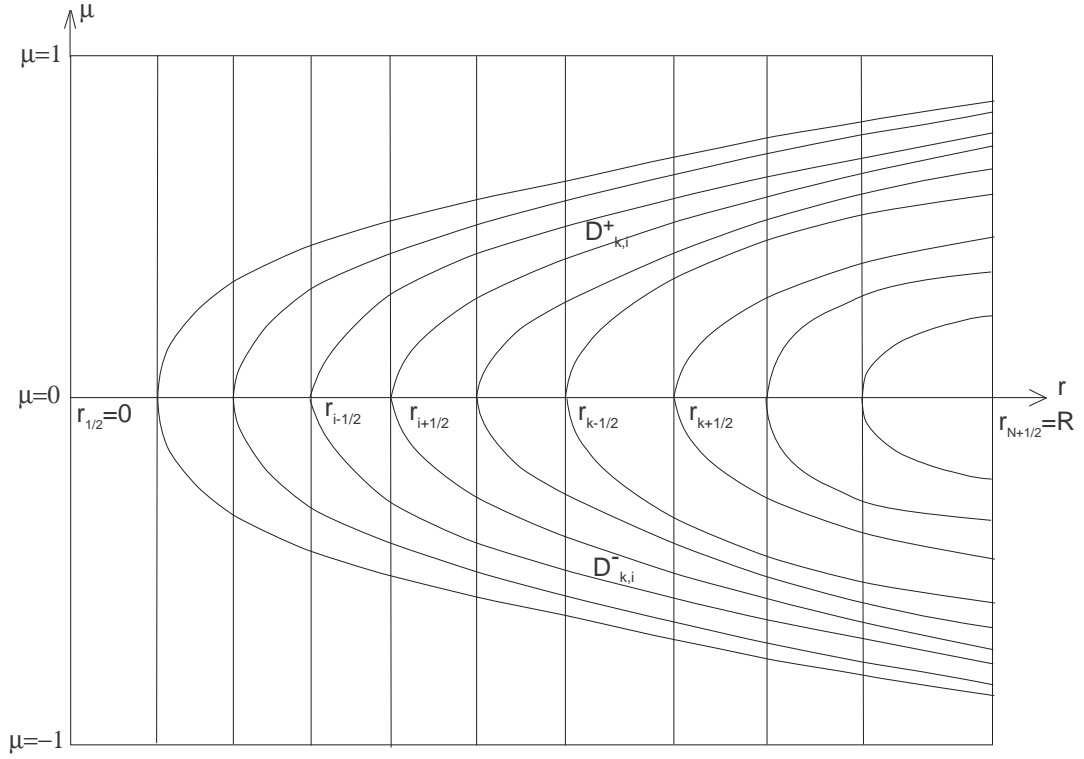
Figure 3.1: The characteristics in (r, μ) coordinates.

where

$$L\psi(r,\mu) \stackrel{def}{=} \mu\frac{\partial}{\partial r}\psi(r,\mu) + \frac{1-\mu^2}{r}\frac{\partial}{\partial\mu}\psi(r,\mu) + \sigma_t(r)\psi(r,\mu)\,, \qquad (3.9)$$

$$Q(r) \stackrel{def}{=} \frac{1}{2}\sigma_s(r)\int_{-1}^{1}\psi(r,\mu')d\mu' + \frac{1}{2}q(r)\,. \qquad (3.10)$$

The corresponding cell C_{ki}^+ in (x,y) coordinates is defined by characteristics (lines) $y = y_{i-1/2}$, $y = y_{i+1/2}$ and arcs of the following concentric circles: $x^2 + y^2 = r_{k-1/2}^2$ and $x^2 + y^2 = r_{k+1/2}^2$ for $x > 0$, i.e. $\mu > 0$ (see Figure 2.2). The balance in C_{ki}^+ cell is defined as

$$\int_{C_{ki}^+} \left(\mathcal{L}\psi(x,y) - \mathcal{Q}(x,y)\right) y\,dy\,dx = 0\,, \qquad (3.11)$$

29

where

$$\mathcal{L}\psi(x,y) \stackrel{def}{=} \frac{\partial}{\partial x}\psi(x,y) + \sigma_t(\sqrt{x^2+y^2})\psi(x,y)\,, \tag{3.12}$$

$$\mathcal{Q}(x,y) \stackrel{def}{=} \frac{1}{2}\sigma_s(\sqrt{x^2+y^2})\phi(\sqrt{x^2+y^2}) + \frac{1}{2}q(\sqrt{x^2+y^2})\,. \tag{3.13}$$

As a result, the balance is given by

$$\int_{y_{i-1/2}}^{y_{i+1/2}} \left[\int_{x_{k-1/2}(y)}^{x_{k+1/2}(y)} (\mathcal{L}\psi(x,y) - \mathcal{Q}(x,y))dx \right] ydy = 0 \,, \text{for } C_{ki}^+ \,\, (\mu > 0)\,, \tag{3.14}$$

$$\int_{y_{i-1/2}}^{y_{i+1/2}} \left[\int_{-x_{k+1/2}(y)}^{-x_{k-1/2}(y)} (\mathcal{L}\psi(x,y) - \mathcal{Q}(x,y))dx \right] ydy = 0 \,, \text{for } C_{ki}^- \,\, (\mu < 0)\,, \tag{3.15}$$

where

$$x_{k-1/2}(y) = \sqrt{r_{k-1/2}^2 - y^2}\,, \tag{3.16}$$

and C_{ki}^- is the cell defined by the same set of circles and characteristic lines as C_{ki}^+ but for

$x < 0$ (i.e. $\mu < 0$). The balance in k^{th} spatial interval $r_{k-1/2} \leq r \leq r_{k+1/2}$ (see Figure 2.2)

is defined as

$$\sum_{i=1}^{k} \int_{C_{ki}^-} (\mathcal{L}\psi(x,y) - \mathcal{Q}(x,y))\, ydydx + \sum_{i=1}^{k} \int_{C_{ki}^+} (\mathcal{L}\psi(x,y) - \mathcal{Q}(x,y))\, ydydx = 0\,, \tag{3.17}$$

and hence

$$\begin{aligned}
&\int_{y_{1/2}}^{y_{k+1/2}} \left[\int_{-x_{k+1/2}(y)}^{-x_{k-1/2}(y)} (\mathcal{L}\psi(x,y) - \mathcal{Q}(x,y))dx \right] ydy \\
&+ \int_{y_{1/2}}^{y_{k+1/2}} \left[\int_{x_{k-1/2}(y)}^{x_{k+1/2}(y)} (\mathcal{L}\psi(x,y) - \mathcal{Q}(x,y))dx \right] ydy = 0\,.
\end{aligned} \tag{3.18}$$

If we use the definition of operators, we get

$$\begin{aligned}
&\int_{y_{1/2}}^{y_{k+1/2}} \left[\int_{-x_{k+1/2}(y)}^{-x_{k-1/2}(y)} \left(\frac{\partial\psi}{\partial x} + \sigma_t\psi - \frac{1}{2}(\sigma_t\phi + q) \right) dx \right] ydy \\
&+ \int_{y_{1/2}}^{y_{k+1/2}} \left[\int_{x_{k-1/2}(y)}^{x_{k+1/2}(y)} \left(\frac{\partial\psi}{\partial x} + \sigma_t\psi - \frac{1}{2}(\sigma_t\phi + q) \right) dx \right] ydy = 0\,.
\end{aligned} \tag{3.19}$$

30

The analysis of Eq. (3.19) shows that the scalar flux averaged over k^{th} spatial interval is

$$\phi_k = \frac{1}{v_k} \int_{y_{1/2}}^{y_{k+1/2}} \left[\int_{-x_{k+1/2}(y)}^{-x_{k-1/2}(y)} \psi(x,y)dx + \int_{x_{k-1/2}(y)}^{x_{k+1/2}(y)} \psi(x,y)dx \right] y \, dy \,, \qquad (3.20)$$

and the net leakage rate in k^{th} spatial interval is given by

$$T_k = \int_{y_{1/2}}^{y_{k+1/2}} (\psi(-x_{k-1/2}(y),y) - \psi(-x_{k+1/2}(y),y) + \psi(x_{k+1/2}(y),y) - \psi(x_{k-1/2}(y),y)) y \, dy \,.$$

$$(3.21)$$

Note that on the other hand we have

$$T_k = r_{k+1/2}^2 J_{k+1/2} - r_{k-1/2}^2 J_{k-1/2} \,. \qquad (3.22)$$

To derive the discrete version of the balance Eq. (3.18) consistent with the transport discretization method under consideration, first we approximate the integration with respect to y and obtain

$$\sum_{i=1}^{k+1} \left[\int_{-x_{k+1/2}(y_{i-1/2})}^{-x_{k-1/2}(y_{i-1/2})} (\mathcal{L}\psi(x,y) - \mathcal{Q}(x,y))dx \right] w_{k,i-1/2}^y$$
$$+ \sum_{i=1}^{k+1} \left[\int_{x_{k-1/2}(y_{i-1/2})}^{x_{k+1/2}(y_{i-1/2})} (\mathcal{L}\psi(x,y) - \mathcal{Q}(x,y))dx \right] w_{k,i-1/2}^y = 0 \,, \qquad (3.23)$$

where

$$\int_{y_{1/2}}^{y_{k+1/2}} f(y) \frac{1}{2} d(y^2) \approx \sum_{i=1}^{k+1} f(y_{i-1/2}) w_{k,i-1/2}^y \,. \qquad (3.24)$$

We use trapezoid rule for numerical integration and get the following weights:

$$w_{k,1/2}^y = \frac{1}{4}(y_{3/2}^2 - y_{1/2}^2) \,, \ i = 1 \,, \qquad (3.25)$$

$$w_{k,i-1/2}^y = \frac{1}{4}(y_{i+1/2}^2 - y_{i-3/2}^2) \,, \ i = 2, ..., k \,,$$

$$w_{k,k+1/2}^y = \frac{1}{4}(y_{k+1/2}^2 - y_{k-1/2}^2) \,, \ i = k+1 \,,$$

$$k = 1, ..., N \,.$$

In case $i = k + 1$ the integration is performed over measure zero, namely, interval of zero length. This leads to no contribution in the sum from the terms with $i = k + 1$. Thus, we have

$$\sum_{i=1}^{k} \left[\int_{-x_{k+1/2}(y_{i-1/2})}^{-x_{k-1/2}(y_{i-1/2})} (\mathcal{L}\psi(x,y) - \mathcal{Q}(x,y))dx \right] w_{k,i-1/2}^{y}$$
$$+ \sum_{i=1}^{k} \left[\int_{x_{k-1/2}(y_{i-1/2})}^{x_{k+1/2}(y_{i-1/2})} (\mathcal{L}\psi(x,y) - \mathcal{Q}(x,y))dx \right] w_{k,i-1/2}^{y} = 0 . \tag{3.26}$$

We now integrate the transport equation along characteristics

$$\int_{-x_{k+1/2}(y_{i-1/2})}^{-x_{k-1/2}(y_{i-1/2})} \mathcal{L}\psi(x,y)dx = \int_{-x_{k+1/2}(y_{i-1/2})}^{-x_{k-1/2}(y_{i-1/2})} \mathcal{Q}(x,y)dx , \quad \text{for } \mu < 0 , \tag{3.27}$$

$$\int_{x_{k-1/2}(y_{i-1/2})}^{x_{k+1/2}(y_{i-1/2})} \mathcal{L}\psi(x,y)dx = \int_{x_{k-1/2}(y_{i-1/2})}^{x_{k+1/2}(y_{i-1/2})} \mathcal{Q}(x,y)dx , \quad \text{for } \mu > 0 . \tag{3.28}$$

It gives rise to

$$\psi_{k-1/2,i-1/2}^{-} - \psi_{k+1/2,i-1/2}^{-} + \int_{x_{k-1/2}(y_{i-1/2})}^{x_{k+1/2}(y_{i-1/2})} \sigma_t(\sqrt{x^2+y^2})\psi^{-}(x,y_{i-1/2})dx =$$
$$\frac{1}{2} \int_{x_{k-1/2}(y_{i-1/2})}^{x_{k+1/2}(y_{i-1/2})} \left(\sigma_s(\sqrt{x^2+y^2})\phi(\sqrt{x^2+y^2}) + q(\sqrt{x^2+y^2}) \right) dx \quad \text{for } \mu < 0 ,$$
$$\tag{3.29}$$

$$\psi_{k+1/2,i-1/2}^{+} - \psi_{k-1/2,i-1/2}^{+} + \int_{x_{k-1/2}(y_{i-1/2})}^{x_{k+1/2}(y_{i-1/2})} \sigma_t(\sqrt{x^2+y^2})\psi^{+}(x,y_{i-1/2})dx =$$
$$\frac{1}{2} \int_{x_{k-1/2}(y_{i-1/2})}^{x_{k+1/2}(y_{i-1/2})} \left(\sigma_s(\sqrt{x^2+y^2})\phi(\sqrt{x^2+y^2}) + q(\sqrt{x^2+y^2}) \right) dx \quad \text{for } \mu > 0 .$$
$$\tag{3.30}$$

The equations (3.1) and (3.3) can be written in the following form:

$$\psi_{k-1/2,i-1/2}^{-} - \psi_{k+1/2,i-1/2}^{-} + \sigma_{t,k}\psi_{k,i-1/2}^{-}\Delta x_{k,i-1/2} = \frac{1}{2}(\sigma_{s,k}\phi_k + q_k)\Delta x_{k,i-1/2} , \quad k = N, ..., i ,$$
$$\tag{3.31}$$

32

$$\psi^+_{k+1/2,i-1/2} - \psi^+_{k-1/2,i-1/2} + \sigma_{t,k}\psi^+_{k,i-1/2}\Delta x_{k,i-1/2} = \frac{1}{2}(\sigma_{s,k}\phi_k+q_k)\Delta x_{k,i-1/2}, \quad k = i, ..., N,$$

$$(3.32)$$

$$\psi^-_{k,i-1/2} = \alpha_{k,i-1/2}\psi^-_{k+1/2,i-1/2} + (1-\alpha_{k,i-1/2})\psi^-_{k-1/2,i-1/2}, \tag{3.33}$$

$$\psi^+_{k,i-1/2} = \alpha_{k,i-1/2}\psi^+_{k-1/2,i-1/2} + (1-\alpha_{k,i-1/2})\psi^+_{k+1/2,i-1/2}, \tag{3.34}$$

$$\alpha_{k,i-1/2} = \frac{1}{\tau_{k,i-1/2}} - \frac{e^{-\tau_{k,i-1/2}}}{1-e^{-\tau_{k,i-1/2}}}, \tag{3.35}$$

where

$$\psi^-_{k,i-1/2} = \frac{1}{\Delta x_{k,i-1/2}}\int_{-x_{k+1/2}(y_{i-1/2})}^{-x_{k-1/2}(y_{i-1/2})} \psi^-(x, y_{i-1/2})dx, \tag{3.36}$$

$$\psi^+_{k,i-1/2} = \frac{1}{\Delta x_{k,i-1/2}}\int_{x_{k-1/2}(y_{i-1/2})}^{x_{k+1/2}(y_{i-1/2})} \psi^+(x, y_{i-1/2})dx, \tag{3.37}$$

are cell-average angular fluxes. From Eqs. (3.26), (3.31), and (3.32) we get

$$\sum_{i=1}^{k}\left[\psi^-_{k-1/2,i-1/2} - \psi^-_{k+1/2,i-1/2} + \sigma_{t,k}\psi^-_{k,i-1/2}\Delta x_{k,i-1/2} - \frac{1}{2}(\sigma_{s,k}\phi_k+q_k)\Delta x_{k,i-1/2}\right]w^y_{k,i-1/2}$$
$$+ \sum_{i=1}^{k}\left[\psi^+_{k+1/2,i-1/2} - \psi^+_{k-1/2,i-1/2} + \sigma_{t,k}\psi^+_{k,i-1/2}\Delta x_{k,i-1/2} - \frac{1}{2}(\sigma_{s,k}\phi_k+q_k)\Delta x_{k,i-1/2}\right]w^y_{k,i-1/2} = 0.$$

$$(3.38)$$

Comparing reaction rates, we see that to derive a conservative method, one needs to define

$$\phi_k\sum_{i=1}^{k}\Delta x_{k,i-1/2}w^y_{k,i-1/2} = \sum_{i=1}^{k}(\psi^-_{k,i-1/2} + \psi^+_{k,i-1/2})\Delta x_{k,i-1/2}w^y_{k,i-1/2}. \tag{3.39}$$

Finally, the *cell-average scalar flux* is defined as

$$\phi_k = \frac{1}{V_k}\sum_{i=1}^{k}(\psi^-_{k,i-1/2} + \psi^+_{k,i-1/2})\Delta x_{k,i-1/2}w^y_{k,i-1/2}, \tag{3.40}$$

$$V_k = \sum_{i=1}^{k}\Delta x_{k,i-1/2}w^y_{k,i-1/2}. \tag{3.41}$$

The discretized net leakage rate is given by

$$\tilde{T}_k = \sum_{i=1}^{k} (\psi^+_{k+1/2,i-1/2} - \psi^+_{k-1/2,i-1/2} + \psi^-_{k-1/2,i-1/2} - \psi^-_{k+1/2,i-1/2}) w^y_{k,i-1/2} \,. \tag{3.42}$$

The analysis of Eq. (3.42) in the form

$$\tilde{T}_k = \sum_{i=1}^{k} (\psi^+_{k+1/2,i-1/2} - \psi^-_{k+1/2,i-1/2}) w^y_{k,i-1/2} - \sum_{i=1}^{k} (\psi^+_{k-1/2,i-1/2} - \psi^-_{k-1/2,i-1/2}) w^y_{k,i-1/2} \,, \tag{3.43}$$

leads to the following definition of the *cell-edge currents*

$$J_{k+1/2} = \frac{1}{r^2_{k+1/2}} \sum_{i=1}^{k} (\psi^+_{k+1/2,i-1/2} - \psi^-_{k+1/2,i-1/2}) w^y_{k,i-1/2} \,. \tag{3.44}$$

Note also that it is equivalent to

$$J_{1/2} = 0 \,, \tag{3.45}$$

$$J_{k+1/2} = \frac{1}{r^2_{k+1/2}} (\tilde{T}_k + r^2_{k-1/2} J_{k-1/2}) \,, \quad k = 1, ..., N \,. \tag{3.46}$$

The balance equation in the kth interval has the following form:

$$\tilde{T}_k + (\sigma_{t,k} - \sigma_{s,k}) V_k \phi_k = q_k V_k \,. \tag{3.47}$$

Hereafter we refer to the proposed method as the conservative method of long characteristics (CMLC) method. The CMLC method is defined by Eqs. (3.31)-(3.35), (3.40), (3.41), and (3.44).

3.1.1 The Asymptotic Diffusion Analysis of CMLC

We define a small parameter ε, introduce scaled cross sections and source

$$\sigma_t = \frac{1}{\varepsilon} \hat{\sigma}_t \,, \quad \sigma_a = \varepsilon \hat{\sigma}_a \,, \quad q = \varepsilon \hat{q} \,, \tag{3.48}$$

34

and consider the transport problem as $\varepsilon \to 0$. Assume that the solution can be expanded in power series of ε

$$\psi^{\pm}_{k-1/2,i-1/2} = \sum_{m=0}^{\infty} \varepsilon^m \psi^{\pm[m]}_{k-1/2,i-1/2} , \quad \psi^{\pm}_{k,i-1/2} = \sum_{m=0}^{\infty} \varepsilon^m \psi^{\pm[m]}_{k,i-1/2} , \quad \phi_k = \sum_{m=0}^{\infty} \varepsilon^m \phi^{[m]}_k ,$$

$$(3.49)$$

and introduce the expansions (3.49) into Eqs. (3.31) and (3.32). We equate the coefficients at powers of ε. This leads to the following $O(\varepsilon^{-1})$ equations

$$\psi^{\pm[0]}_{k,i-1/2} = \frac{1}{2}\phi^{[0]} ,$$

$$(3.50)$$

$O(1)$ equations

$$\psi^{-[0]}_{k-1/2,i-1/2} - \psi^{-[0]}_{k+1/2,i-1/2} + \hat{\sigma}_t \Delta x_{k,i-1/2}\psi^{-[1]}_{k,i-1/2} = \frac{1}{2}\hat{\sigma}_t \Delta x_{k,i-1/2}\phi^{[1]}_k ,$$

$$(3.51)$$

$$\psi^{+[0]}_{k+1/2,i-1/2} - \psi^{+[0]}_{k-1/2,i-1/2} + \hat{\sigma}_t \Delta x_{k,i-1/2}\psi^{+[1]}_{k,i-1/2} = \frac{1}{2}\hat{\sigma}_t \Delta x_{k,i-1/2}\phi^{[1]}_k ,$$

$$(3.52)$$

$O(\varepsilon)$ equations

$$\psi^{-[1]}_{k-1/2,i-1/2} - \psi^{-[1]}_{k+1/2,i-1/2} + \hat{\sigma}_t \Delta x_{k,i-1/2}\psi^{-[2]}_{k,i-1/2} = \frac{1}{2}\Delta x_{k,i-1/2}\left(\hat{\sigma}_t\psi^{[2]}_k - \hat{\sigma}_a\phi^{[1]}_k + \hat{q}\right) ,$$

$$(3.53)$$

$$\psi^{+[1]}_{k+1/2,i-1/2} - \psi^{+[1]}_{k-1/2,i-1/2} + \hat{\sigma}_t \Delta x_{k,i-1/2}\psi^{+[2]}_{k,i-1/2} = \frac{1}{2}\Delta x_{k,i-1/2}\left(\hat{\sigma}_t\psi^{[2]}_k - \hat{\sigma}_a\phi^{[1]}_k + \hat{q}\right) .$$

$$(3.54)$$

We now introduce series (3.49) into Eqs. (3.33) and (3.34) to get

$$\psi^{-[0]}_{k,i-1/2} = \psi^{-[0]}_{k-1/2,i-1/2} ,$$

$$(3.55)$$

$$\psi^{+[0]}_{k,i-1/2} = \psi^{+[0]}_{k+1/2,i-1/2} .$$

$$(3.56)$$

This gives rise to

$$\psi^{-[0]}_{k-1/2,i-1/2} = \frac{1}{2}\phi^{[0]}_k ,$$

$$(3.57)$$

35

$$\psi_{k+1/2,i-1/2}^{+[0]} = \frac{1}{2}\phi_k^{[0]} \, . \tag{3.58}$$

Note that from Eq. (3.40) we have

$$\phi_k^{[m]} = \frac{1}{V_k}\sum_{i=0}^{k}(\psi_{k,i-1/2}^{-[m]} + \psi_{k,i-1/2}^{+[m]})\Delta x_{k,i-1/2}w_{k,i-1/2}^{y} \, . \tag{3.59}$$

First, we analyze the equations in the interior of the problem domain. The equations (3.51) and (3.52) are added together and summed with weights $w_{k,i-1/2}^{y}$ over $1 \leq i \leq k$. Taking into account Eqs. (3.59) and (3.41), we get

$$\sum_{i=1}^{k}(\psi_{k+1/2,i-1/2}^{+[0]} - \psi_{k-1/2,i-1/2}^{+[0]} + \psi_{k-1/2,i-1/2}^{-[0]} - \psi_{k+1/2,i-1/2}^{-[0]})w_{k,i-1/2}^{y} = 0 \, . \tag{3.60}$$

Using Eqs. (3.57) and (3.58), we obtain that

$$\frac{1}{2}\sum_{i=1}^{k}(\phi_k^{[0]} - \phi_{k+1}^{[0]})w_{k,i-1/2}^{y} - \frac{1}{2}\sum_{i=1}^{k}(\phi_{k-1}^{[0]} - \phi_k^{[0]})w_{k,i-1/2}^{y} = 0 \, . \tag{3.61}$$

This leads to the following approximation of the diffusion equation in interior cells:

$$\left(\phi_k^{[0]} - \phi_{k+1}^{[0]}\right) - \left(\phi_{k-1}^{[0]} - \phi_k^{[0]}\right) = 0 \, , \quad k = 1, ..., N-1 \, . \tag{3.62}$$

We now consider the boundary cell to determine the asymptotic boundary condition. In the Nth cell, Eq. (3.60) is given by

$$\sum_{i=1}^{N}(\psi_{N+1/2,i-1/2}^{+[0]} - \psi_{N-1/2,i-1/2}^{+[0]} + \psi_{N-1/2,i-1/2}^{-[0]} - \psi_{N+1/2,i-1/2}^{-[0]})w_{N,i-1/2}^{y} = 0 \, , \tag{3.63}$$

and hence

$$\frac{1}{2}\sum_{i=1}^{N}(\phi_N^{[0]} - \phi_{N-1}^{[0]} + \phi_N^{[0]} - 2\psi_{i-1/2}^{in})w_{N,i-1/2}^{y} = 0 \, . \tag{3.64}$$

As a result, we have

$$\left(\phi_N^{[0]} - \frac{2}{F}\sum_{i=1}^{N}\psi_{i-1/2}^{in}w_{N,i-1/2}^{y}\right) - \left(\phi_{N-1}^{[0]} - \phi_N^{[0]}\right) = 0 \, , \tag{3.65}$$

36

where

$$F = \sum_{i=1}^{N} w^{y}_{N,i-1/2}.$$ (3.66)

Thus, the asymptotic boundary condition of CMLC is defined as

$$\phi_{N+1}^{[0]} = \frac{2}{F} \sum_{i=1}^{N} \psi_{i-1/2}^{in} w^{y}_{N,i-1/2}.$$ (3.67)

We notice that the CMLC method gives a discretized diffusion equation similar to those derived in Vladimirov's methods. The resulting equation does not have an external source and does not depend on material cross sections. The boundary condition given in this case resembles a discretized version of the weighted integral given in the continuous form in section 1.3. The CMLC equations do not lead to an accurate discretization of the diffusion equation in the thick-diffusion limit. This result is similar to one of the step characteristics method in 1D slab geometry. These conclusions are confirmed in the numerical results chapter of this thesis.

3.2 Linear Long Characteristic Method

In this section we formulate a linear characteristic method in (x, y) variables that is based on ideas of a method for slab geometry. Now, approximating the total source with a linear function and integrating Eq. (2.8) over the interval $x_{k+1/2,i-1/2} \leq x \leq x_{k-1/2,i-1/2}$ yields the balance equation for $\mu \geq 0$

$$\psi^{+}_{k+1/2,i-1/2} - \psi^{+}_{k-1/2,i-1/2} + \sigma_{t,k} \psi^{+}_{k,i-1/2} \Delta x_{k,i-1/2} = \hat{Q}_{k,i-1/2} \Delta x_{k,i-1/2},$$ (3.68)

where

$$\hat{Q}_{k,i-1/2} = \frac{1}{\Delta x_{k,i-1/2}} \int_{x_{k-1/2,i-1/2}}^{x_{k+1/2,i-1/2}} Q(x, y_{i-1/2})) dx.$$ (3.69)

37

Integrating Eq. (2.8) over the interval $-x_{k+1/2,i-1/2} \leq x \leq -x_{k-1/2,i-1/2}$ yields the balance equation for $\mu \leq 0$

$$\psi^-_{k-1/2,i-1/2} - \psi^-_{k+1/2,i-1/2} + \sigma_{t,k}\psi^-_{k,i-1/2}\Delta x_{k,i-1/2} = \hat{Q}_{k,i-1/2}\Delta x_{k,i-1/2}\,. \tag{3.70}$$

Now, we integrate Eq. (2.8) over $x_{k+1/2,i-1/2} \leq x \leq x_{k-1/2,i-1/2}$ with the weight

$$\frac{6}{\Delta x^2_{k,i-1/2}}(x - \bar{x}_{k,i-1/2})\,, \tag{3.71}$$

where

$$\bar{x}_{k,i-1/2} = \frac{1}{2}(x_{k+1/2,i-1/2} + x_{k-1/2,i-1/2})\,, \tag{3.72}$$

to obtain the first spatial moment of the transport equation for values of $\mu \geq 0$

$$3\,(\psi^+_{k+1/2,i-1/2} + \psi^+_{k+1/2,i-1/2} - 2\psi^+_{k,i-1/2}) + \sigma_{t,k}\psi^{x,+}_{k,i-1/2}\Delta x_{k,i-1/2} = \hat{Q}^x_{k,i-1/2}\Delta x_{k,i-1/2}\,, \tag{3.73}$$

where

$$\psi^{x,+}_{k,i-1/2} = \frac{6}{\Delta x^2_{k,i-1/2}}\int_{x_{k-1/2,i-1/2}}^{x_{k+1/2,i-1/2}}(x - \bar{x}_{k,i-1/2})\psi(x, y_{i-1/2})dx\,, \tag{3.74}$$

$$\hat{Q}^x_{k,i-1/2} = \frac{6}{\Delta x^2_{k,i-1/2}}\int_{x_{k-1/2,i-1/2}}^{x_{k+1/2,i-1/2}}(x - \bar{x}_{k,i-1/2})Q(x, y_{i-1/2})dx\,. \tag{3.75}$$

For $\mu \leq 0$, we integrate Eq. (2.8) over $-x_{k+1/2,i-1/2} \leq x \leq -x_{k-1/2,i-1/2}$ with the following weight

$$\frac{6}{\Delta x^2_{k,i-1/2}}(x + \bar{x}_{k,i-1/2})\,, \tag{3.76}$$

and get

$$3\,(\psi^-_{k+1/2,i-1/2} + \psi^-_{k+1/2,i-1/2} - 2\psi^-_{k,i-1/2}) + \sigma_{t,k}\psi^{x,-}_{k,i-1/2}\Delta x_{k,i-1/2} = -\hat{Q}^x_{k,i-1/2}\Delta x_{k,i-1/2}\,, \tag{3.77}$$

where

$$\psi_{k,i-1/2}^{x,-} = \frac{6}{\Delta x_{k,i-1/2}^2} \int_{-x_{k-1/2,i-1/2}}^{-x_{k+1/2,i-1/2}} (x + \bar{x}_{k,i-1/2})\psi(x, y_{i-1/2})dx\,. \tag{3.78}$$

We make the following assumptions for the source terms:

$$\hat{Q}_{k,i-1/2} = Q_k\,, \tag{3.79}$$

$$\hat{Q}_{k,i-1/2}^x = Q_k^x\,.$$

Thus, we have the following set of discretized equations

$$\psi_{k+1/2,i-1/2}^+ - \psi_{k-1/2,i-1/2}^+ + \sigma_{t,k}\psi_{k,i-1/2}^+\Delta x_{k,i-1/2} = Q_k\Delta x_{k,i-1/2}\,, \tag{3.80}$$

$$\psi_{k-1/2,i-1/2}^- - \psi_{k+1/2,i-1/2}^- + \sigma_{t,k}\psi_{k,i-1/2}^-\Delta x_{k,i-1/2} = Q_k\Delta x_{k,i-1/2}\,, \tag{3.81}$$

$$3\,(\psi_{k+1/2,i-1/2}^- + \psi_{k+1/2,i-1/2}^- - 2\psi_{k,i-1/2}^-) + \sigma_{t,k}\psi_{k,i-1/2}^{x,-}\Delta x_{k,i-1/2} = Q_k^x\Delta x_{k,i-1/2}\,, \tag{3.82}$$

$$3\,(\psi_{k+1/2,i-1/2}^- + \psi_{k+1/2,i-1/2}^- - 2\psi_{k,i-1/2}^-) + \sigma_{t,k}\psi_{k,i-1/2}^{x,-}\Delta x_{k,i-1/2} = -Q_k^x\Delta x_{k,i-1/2}\,, \tag{3.83}$$

where

$$Q_k = \frac{1}{2}(\sigma_{s,k}\phi_k + q_k)\,, \tag{3.84}$$

$$Q_k^x = \frac{1}{2}(\sigma_{s,k}\phi_k^x + q_k^x)\,.$$

To define the cell-averaged scalar flux, ϕ_k, we add Eq. (3.80) and Eq. (3.81) multiplied by

the weights $w_{k,i-1/2}^y$, and sum over all cells

$$\sum_{i=1}^{k} \left[\psi_{k+1/2,i-1/2}^+ - \psi_{k-1/2,i-1/2}^+ + \psi_{k-1/2,i-1/2}^- - \psi_{k+1/2,i-1/2}^-\right] w_{k,i-1/2}^y +$$

$$\sigma_{t,k}\sum_{i=1}^{k} \left[(\psi_{k,i-1/2}^+ + \psi_{k,i-1/2}^-)\Delta x_{k,i-1/2}\right] w_{k,i-1/2}^y = (\sigma_{s,k}\phi_k + q_k)\sum_{i=1}^{k}\Delta x_{k,i-1/2}w_{k,i-1/2}^y\,.$$

$$\tag{3.85}$$

Comparing reaction rates, we have

$$\phi_k = \frac{1}{V_k} \sum_{i=1}^{k} (\psi_{k,i-1/2}^{+} + \psi_{k,i-1/2}^{-}) \Delta x_{k,i-1/2} w_{k,i-1/2}^{y}. \tag{3.86}$$

Furthermore, we define the first spatial moment of the scalar flux, ϕ_k^x, by subtracting Eq. (3.82) from Eq. (3.83), multiplying by the weights $w_{k,i-1/2}^{y}$, and summing over all cells. As a result we get

$$\phi_k^x = \frac{1}{V_k} \sum_{i=1}^{k} (\psi_{k,i-1/2}^{x,+} - \psi_{k,i-1/2}^{x,-}) \Delta x_{k,i-1/2} w_{k,i-1/2}^{y}. \tag{3.87}$$

Note that the cell-edge currents are defined by Eq. (3.44). We now approximate the scalar flux in each cell by the following linear function:

$$\phi_k(x) = \begin{cases} \phi_k + \frac{2}{\Delta x_{k,i-1/2}}(x - \bar{x}_{k,i-1/2})\phi_k^x, & x_{k-1/2,i-1/2} \leq x \leq x_{k+1/2,i-1/2} \\ \\ \phi_k - \frac{2}{\Delta x_{k,i-1/2}}(x + \bar{x}_{k,i-1/2})\phi_k^x, & -x_{k+1/2,i-1/2} \leq x \leq -x_{k-1/2,i-1/2} \end{cases}, \tag{3.88}$$

and evaluate Eq. (2.10) at $x = -x_{k-1/2,i-1/2}$, $x_o = -x_{k+1/2,i-1/2}$, and $y_{i-1/2}$ to get

$$\begin{aligned} \psi_{k-1/2,i-1/2}^{-} = \psi_{k+1/2,i-1/2}^{-} e^{-\tau_{k,i-1/2}} + \frac{1}{2\sigma_{t,k}}(1 - e^{-\tau_{k,i-1/2}})Q_k \\ - \frac{1}{\sigma_{t,k}\tau_{k,i-1/2}} \left[\frac{\tau_{k,i-1/2}}{2}(1 + e^{-\tau_{k,i-1/2}}) + e^{-\tau_{k,i-1/2}} - 1 \right] Q_k^x, \end{aligned} \tag{3.89}$$

where

$$\psi_{N+1/2,i-1/2}^{-} = \psi^{in}(y_{i-1/2}), \tag{3.90}$$

$$k = N, ..., i.$$

Evaluating Eq. (2.10) at $x = x_{k+1/2,i-1/2}$, $x_o = x_{k-1/2,i-1/2}$, and $y_{i-1/2}$ yields

$$\begin{aligned} \psi_{k+1/2,i-1/2}^{+} = \psi_{k-1/2,i-1/2}^{+} e^{-\sigma_{t,k}\Delta x_{k,i-1/2}} + \frac{1}{2\sigma_{t,k}}(1 - e^{-\tau_{k,i-1/2}})Q_k \\ + \frac{1}{\sigma_{t,k}\tau_{k,i-1/2}} \left[\frac{\tau_{k,i-1/2}}{2}(1 + e^{-\tau_{k,i-1/2}}) + e^{-\tau_{k,i-1/2}} - 1 \right] Q_k^x, \end{aligned} \tag{3.91}$$

40

where

$$\psi^+_{i-1/2,i-1/2} = \psi^-_{i-1/2,i-1/2} \,, \tag{3.92}$$

$$k = i, .., N \,,$$

$$\text{for} \quad i = 1, ..., N+1 \,.$$

Hereafter we refer to the proposed method as Linear Long Characteristic method (LLCM).

The LLCM is defined by Eqs. (3.80)-(3.84), (3.89)-(3.92), (3.86), (3.87).

3.2.1 The Asymptotic Diffusion Analysis of LLCM

We define a small parameter ε, introduce scaled cross sections and source

$$\sigma_t = \frac{1}{\varepsilon}\hat{\sigma}_t \,, \quad \sigma_a = \varepsilon\hat{\sigma}_a \,, \quad q = \varepsilon\hat{q} \,, \tag{3.93}$$

and consider the transport problem as $\varepsilon \to 0$. Assume that the solution can be expanded

in power series of ε

$$\psi^\pm_{k-1/2,i-1/2} = \sum_{m=0}^{\infty} \varepsilon^m \psi^{\pm[m]}_{k-1/2,i-1/2} \,, \quad \psi^\pm_{k,i-1/2} = \sum_{m=0}^{\infty} \varepsilon^m \psi^{\pm[m]}_{k,i-1/2} \,, \quad \psi^{x\pm}_{k,i-1/2} = \sum_{m=0}^{\infty} \varepsilon^m \psi^{x\pm[m]}_{k,i-1/2} \,,$$

$$\phi_k = \sum_{m=0}^{\infty} \varepsilon^m \phi^{[m]}_k \,, \quad \phi^x_k = \sum_{m=0}^{\infty} \varepsilon^m \phi^{x[m]}_k \,,$$

$$\tag{3.94}$$

and introduce the expansions (3.94) into Eqs. (3.80)-(3.84), (3.89), (3.90). We equate the

coefficients at powers of ε. This leads to the following sets of equations

$O(\varepsilon^{-1})$ equations

$$\psi^{\pm[0]}_{k,i-1/2} = \frac{1}{2}\phi^{[0]}_k \,, \tag{3.95}$$

$$\psi_{k,i-1/2}^{x,\pm[0]} = \pm\frac{1}{2}\phi_k^{[0]}\,, \tag{3.96}$$

$O(1)$ equations

$$\psi_{k-1/2,i-1/2}^{-[0]} = \frac{1}{2}\phi_k^{[0]} - \frac{1}{2}\phi_k^{x[0]}\,, \tag{3.97}$$

$$\psi_{k+1/2,i-1/2}^{+[0]} = \frac{1}{2}\phi_k^{[0]} + \frac{1}{2}\phi_k^{x[0]}\,, \tag{3.98}$$

$$\psi_{k+1/2,i-1/2}^{+[0]} - \psi_{k-1/2,i-1/2}^{+[0]} + \hat{\sigma}_{t,k}\Delta x_{k,i-1/2}\psi_{k,i-1/2}^{+[1]} = \frac{1}{2}\hat{\sigma}_{t,k}\Delta x_{k,i-1/2}\phi_k^{[1]}\,, \tag{3.99}$$

$$\psi_{k-1/2,i-1/2}^{-[0]} - \psi_{k+1/2,i-1/2}^{-[0]} + \hat{\sigma}_{t,k}\Delta x_{k,i-1/2}\psi_{k,i-1/2}^{-[1]} = \frac{1}{2}\hat{\sigma}_{t,k}\Delta x_{k,i-1/2}\phi_k^{[1]}\,, \tag{3.100}$$

$$3\,(\psi_{k+1/2,i-1/2}^{+[0]} + \psi_{k-1/2,i-1/2}^{+[0]} - 2\psi_{k,i-1/2}^{+[0]}) + \hat{\sigma}_{t,k}\Delta x_{k,i-1/2}\psi_{k,i-1/2}^{+x[1]} = \frac{1}{2}\hat{\sigma}_{t,k}\Delta x_{k,i-1/2}\phi_k^{x[1]}\,, \tag{3.101}$$

$$3\,(\psi_{k-1/2,i-1/2}^{-[0]} + \psi_{k+1/2,i-1/2}^{-[0]} - 2\psi_{k,i-1/2}^{-[0]}) + \hat{\sigma}_{t,k}\Delta x_{k,i-1/2}\psi_{k,i-1/2}^{-x[1]} = -\frac{1}{2}\hat{\sigma}_{t,k}\Delta x_{k,i-1/2}\phi_k^{x[1]}\,, \tag{3.102}$$

$O(\varepsilon)$ equations

$$\psi_{k,i-1/2}^{-[1]} = \frac{1}{2}\phi_k^{[1]} - \frac{1}{2}\phi_k^{x[1]} + \frac{1}{\hat{\sigma}_{t,k}\Delta x_{k,i-1/2}}\phi_k^{x[0]}\,, \tag{3.103}$$

$$\psi_{k,i-1/2}^{+[1]} = \frac{1}{2}\phi_k^{[1]} + \frac{1}{2}\phi_k^{x[1]} - \frac{1}{\hat{\sigma}_{t,k}\Delta x_{k,i-1/2}}\phi_k^{x[0]}\,, \tag{3.104}$$

$$\psi_{k-1/2,i-1/2}^{-[1]} - \psi_{k+1/2,i-1/2}^{-[1]} + \hat{\sigma}_{t,k}\Delta x_{k,i-1/2}\psi_{k,i-1/2}^{-[2]} =$$
$$\frac{1}{2}\hat{\sigma}_{t,k}\Delta x_{k,i-1/2}\phi_k^{[2]} - \frac{1}{2}\hat{\sigma}_{a,k}\Delta x_{k,i-1/2}\phi_k^{[0]} + \frac{1}{2}\hat{q}_k\Delta x_{k,i-1/2}\,, \tag{3.105}$$

$$\psi_{k+1/2,i-1/2}^{+[1]} - \psi_{k-1/2,i-1/2}^{+[1]} + \hat{\sigma}_{t,k}\Delta x_{k,i-1/2}\psi_{k,i-1/2}^{+[2]} =$$
$$\frac{1}{2}\hat{\sigma}_{t,k}\Delta x_{k,i-1/2}\phi_k^{[2]} - \frac{1}{2}\hat{\sigma}_{a,k}\Delta x_{k,i-1/2}\phi_k^{[0]} + \frac{1}{2}\hat{q}_k\Delta x_{k,i-1/2}\,, \tag{3.106}$$

$$3\left(\psi_{k-1/2,i-1/2}^{-[1]} + \psi_{k+1/2,i-1/2}^{-[1]} - 2\psi_{k,i-1/2}^{-[1]}\right) + \hat{\sigma}_{t,k}\Delta x_{k,i-1/2}\psi_{k,i-1/2}^{-x[2]} =$$

$$-\frac{1}{2}\hat{\sigma}_{t,k}\Delta x_{k,i-1/2}\phi_k^{x[2]} + \frac{1}{2}\hat{\sigma}_{a,k}\Delta x_{k,i-1/2}\phi^{x[0]} - \frac{1}{2}\hat{q}_k^x \Delta x_{k,i-1/2},$$

$$(3.107)$$

$$3\left(\psi_{k+1/2,i-1/2}^{+[1]} + \psi_{k-1/2,i-1/2}^{+[1]} - 2\psi_{k,i-1/2}^{+[1]}\right) + \hat{\sigma}_{t,k}\Delta x_{k,i-1/2}\psi_{k,i-1/2}^{+x[2]} =$$

$$\frac{1}{2}\hat{\sigma}_{t,k}\Delta x_{k,i-1/2}\phi_k^{x[2]} - \frac{1}{2}\hat{\sigma}_{a,k}\Delta x_{k,i-1/2}\phi^{x[0]} + \frac{1}{2}\hat{q}_k^x \Delta x_{k,i-1/2}.$$

$$(3.108)$$

First, we analyze the equations in the interior of the problem domain. The equations (3.99) and (3.100) are added and summed with weights $w_{k,i-1/2}^y$ over $1 \leq i \leq k$ and we get

$$\sum_{i=1}^{k}\left(\psi_{k+1/2,i-1/2}^{+[0]} - \psi_{k-1/2,i-1/2}^{+[0]} + \psi_{k-1/2,i-1/2}^{-[0]} - \psi_{k+1/2,i-1/2}^{-[0]}\right)w_{k,i-1/2}^y = 0. \qquad (3.109)$$

Subtracting Eq. (3.101) from (3.102) and summing with weights $w_{k,i-1/2}^y$ over $1 \leq i \leq k$ we obtain

$$3\sum_{i=1}^{k}\left[\psi_{k+1/2,i-1/2}^{+[0]} + \psi_{k-1/2,i-1/2}^{+[0]} - \psi_{k-1/2,i-1/2}^{-[0]} - \psi_{k+1/2,i-1/2}^{-[0]}\right.$$

$$\left. + 2(\psi_{k,i-1/2}^{+[0]} - \psi_{k,i-1/2}^{-[0]})\right]w_{k,i-1/2}^y = 0.$$

$$(3.110)$$

Substituting Eq. (3.95) and (3.96) into Eq. (3.110) yields

$$\sum_{i=1}^{k}\left(\psi_{k+1/2,i-1/2}^{+[0]} + \psi_{k-1/2,i-1/2}^{+[0]} - \psi_{k+1/2,i-1/2}^{-[0]} - \psi_{k-1/2,i-1/2}^{-[0]}\right)w_{k,i-1/2}^y = 0. \qquad (3.111)$$

Equations (3.109) and (3.111) lead to the following relationships

$$\sum_{i=1}^{k}\left(\psi_{k+1/2,i-1/2}^{+[0]} - \psi_{k+1/2,i-1/2}^{-[0]}\right)w_{k,i-1/2}^y = 0, \qquad (3.112)$$

$$\sum_{i=1}^{k}\left(\psi_{k-1/2,i-1/2}^{+[0]} - \psi_{k-1/2,i-1/2}^{-[0]}\right)w_{k,i-1/2}^y = 0. \qquad (3.113)$$

Now, we define asymptotic cell edge scalar fluxes. Substituting Eqs. (3.97) and (3.98) into Eq. (3.112) gives

$$(\phi_k^{[0]} + \phi_k^{x[0]}) = (\phi_{k+1}^{[0]} - \phi_{k+1}^{x[0]}) \,, \tag{3.114}$$

and, substituting Eqs. (3.97) and (3.98) into Eq. (3.113) gives

$$(\phi_{k-1}^{[0]} + \phi_{k-1}^{x[0]}) = (\phi_k^{[0]} - \phi_k^{x[0]}) \,. \tag{3.115}$$

Using Eqs. (3.114) and (3.115), we define

$$\phi_{k+1/2}^{[0]} \stackrel{\text{def}}{=} (\phi_k^{[0]} + \phi_k^{x[0]}) \,, \tag{3.116}$$

$$\phi_{k-1/2}^{[0]} \stackrel{\text{def}}{=} (\phi_k^{[0]} - \phi_k^{x[0]}) \,. \tag{3.117}$$

Furthermore, Eq. (3.116) and Eq. (3.117) yield the following relationships

$$\phi_k^{[0]} = \frac{1}{2}(\phi_{k+1/2}^{[0]} + \phi_{k-1/2}^{[0]}) \,, \tag{3.118}$$

$$\phi_k^{x[0]} = \frac{1}{2}(\phi_{k+1/2}^{[0]} - \phi_{k-1/2}^{[0]}) \,, \tag{3.119}$$

and using Eqs. (3.97) and (3.98)

$$\psi_{k+1/2,i-1/2}^{+[0]} = \frac{1}{2}\phi_{k+1/2}^{[0]} \,, \quad k = 1, ..., N-1 \,, \tag{3.120}$$

$$\psi_{k-1/2,i-1/2}^{-[0]} = \frac{1}{2}\phi_{k-1/2}^{[0]} \,, \quad k = 1, ..., N-1 \,. \tag{3.121}$$

Now, subtracting Eq. (3.99) from Eq. (3.100) and summing with weights $w_{k,i-1/2}^y$ over $1 \le i \le k$ gives

$$r_k^2 J_k^{[1]} = -\frac{1}{\hat{\sigma}_{t,k}} \sum_{i=1}^{k} \frac{1}{\Delta x_{k,i-1/2}} \left(\psi_{k+1/2,i-1/2}^{+[0]} - \psi_{k-1/2,i-1/2}^{+[0]} \right.$$

$$\left. - \psi_{k-1/2,i-1/2}^{-[0]} + \psi_{k+1/2,i-1/2}^{-[0]} \right) w_{k,i-1/2}^y \,,$$

$$\tag{3.122}$$

where the cell-averaged current is defined by

$$r_k^2 J_k^{[1]} = \sum_{i=1}^{k} \left(\psi_{k,i-1/2}^{+[1]} - \psi_{k,i-1/2}^{-[1]} \right) w_{k,i-1/2}^y \,. \tag{3.123}$$

Substituting in Eq. (3.120) and (3.121) leads to the following condition

$$r_k^2 J_k^{[1]} = -\frac{1}{\hat{\sigma}_{t,k}} \left(\phi_{k+1/2}^{[0]} - \phi_{k-1/2}^{[0]} \right) \sum_{i=1}^{k} \frac{w_{k,i-1/2}^y}{\Delta x_{k,i-1/2}} \,. \tag{3.124}$$

Now, we add Eqs. (3.105) and (3.106) and sum with weights $w_{k,i-1/2}^y$ over $1 \leq i \leq k$

$$\sum_{i=1}^{k} \left(\psi_{k-1/2,i-1/2}^{-[1]} - \psi_{k+1/2,i-1/2}^{-[1]} + \psi_{k-1/2,i-1/2}^{+[1]} - \psi_{k+1/2,i-1/2}^{+[1]} \right) w_{k,i-1/2}^y + \hat{\sigma}_{a,k} \phi_k^{[0]} V_k = \hat{q}_k V_k \,.$$

$$\tag{3.125}$$

Using Eq. (3.44), we get

$$r_{k+1/2}^2 J_{k+1/2}^{[1]} - r_{k-1/2}^2 J_{k-1/2}^{[1]} = -\hat{\sigma}_{a,k} \phi_k^{[0]} V_k + \hat{q}_k V_k \,. \tag{3.126}$$

Finally, we subtract Eqs. (3.107) from (3.108) and sum with weights $w_{k,i-1/2}^y$ over $1 \leq i \leq k$

$$\sum_{i=1}^{k} 3 \left(-\psi_{k+1/2,i-1/2}^{-[1]} - \psi_{k-1/2,i-1/2}^{-[1]} + \psi_{k-1/2,i-1/2}^{+[1]} + \psi_{k+1/2,i-1/2}^{+[1]} \right) w_{k,i-1/2}^y -$$

$$\sum_{i=1}^{k} 2(\psi_{k,i-1/2}^{+[1]} - \psi_{k,i-1/2}^{-[1]}) w_{k,i-1/2}^y = -\hat{\sigma}_{a,k} \phi_k^{x[0]} V_k + \hat{q}_k^x V_k \,, \tag{3.127}$$

and using Eqs. (3.44) and (3.124) we obtain

$$r_{k+1/2}^2 J_{k+1/2}^{[1]} + r_{k-1/2}^2 J_{k-1/2}^{[1]} - 2r_k^2 J_k^{[1]} = -\frac{1}{3}\hat{\sigma}_{a,k} \phi_k^{x[0]} V_k + \frac{1}{3}\hat{q}_k^x V_k \,. \tag{3.128}$$

Adding Eq. (3.126) evaluated at k and Eq. (3.126) evaluated at $k+1$ and subtracting Eq. (3.128) evaluated at k from Eq. (3.128) evaluated at $k+1$ gives

$$r_{k+3/2}^2 J_{k+3/2}^{[1]} - r_{k-1/2}^2 J_{k-1/2}^{[1]} = -\hat{\sigma}_{a,k+1} \phi_{k+1}^{[0]} V_{k+1} - \hat{\sigma}_{a,k} \phi_k^{[0]} V_k + \hat{q}_{k+1} V_{k+1} + \hat{q}_k V_k \,, \tag{3.129}$$

$$r_{k+3/2}^2 J_{k+3/2}^{[1]} - r_{k-1/2}^2 J_{k-1/2}^{[1]} - 2(r_{k+1}^2 J_{k+1}^{[1]} - r_k^2 J_k^{[1]}) =$$

$$-\frac{1}{3}(\hat{\sigma}_{a,k+1}\phi_{k+1}^{x[0]} V_{k+1} - \hat{\sigma}_{a,k}\phi_k^{x[0]} V_k) + \frac{1}{3}(\hat{q}_{k+1}^x V_{k+1} - \hat{q}_k^x V_k).$$

$$(3.130)$$

Equating Eqs. (3.129) and (3.130) and substituting in Eqs. (3.119), (3.118), and (3.124) yields the discrete diffusion equation for the leading order solution in the interior of the problem.

$$-\frac{1}{\hat{\sigma}_{t,k+1}}\left(\phi_{k+3/2}^{[0]} - \phi_{k+1/2}^{[0]}\right)\sum_{i=1}^{k+1}\frac{w_{k+1,i-1/2}^y}{\Delta x_{k+1,i-1/2}} + \frac{1}{\hat{\sigma}_{t,k}}\left(\phi_{k+1/2}^{[0]} - \phi_{k-1/2}^{[0]}\right)\sum_{i=1}^{k+1}\frac{w_{k,i-1/2}^y}{\Delta x_{k+1,i-1/2}} +$$

$$\frac{1}{4}\hat{\sigma}_{a,k}V_k\left(\frac{4}{3}\phi_{k+1/2}^{[0]} + \frac{2}{3}\phi_{k-1/2}^{[0]}\right) + \frac{1}{4}\hat{\sigma}_{a,k+1}V_{k+1}\left(\frac{4}{3}\phi_{k+1/2}^{[0]} + \frac{2}{3}\phi_{k+3/2}^{[0]}\right) =$$

$$\frac{1}{2}V_k\left(\hat{q}_k + \frac{1}{3}\hat{q}_k^x\right) + \frac{1}{2}V_{k+1}\left(\hat{q}_{k+1} - \frac{1}{3}\hat{q}_{k+1}^x\right).$$

$$(3.131)$$

We see that LLCM limits to a three-point discretized version of the diffusion equation for the leading order solution.

Now, we consider the reflecting boundary condition in cell $k = 1$, where $J_{1/2}^{[1]} = 0$. Equations (3.126) and (3.128) become

$$r_{3/2}^2 J_{3/2}^{[1]} = -\hat{\sigma}_{a,1}\phi_1^{[0]} V_1 + \hat{q}_1 V_1, \tag{3.132}$$

$$r_{3/2}^2 J_{3/2}^{[1]} - 2r_1^2 J_1^{[1]} = -\frac{1}{3}\hat{\sigma}_{a,1}\phi_1^{x[0]} V_1 + \frac{1}{3}\hat{q}_1^x V_1. \tag{3.133}$$

Equating Eqs. (3.132) and (3.133) and substituting in Eqs. (3.118), (3.119), and (3.124) yields the discrete diffusion equation in terms of the leading order solution for the center boundary of the problem

$$\frac{1}{2\hat{\sigma}_{t,1}}\left(\phi_{3/2}^{[0]} - \phi_{1/2}^{[0]}\right)\frac{w_{1,1/2}^y}{\Delta x_{1,1/2}} = \frac{1}{4}\hat{\sigma}_{a,1}V_1\left(\frac{4}{3}\phi_{3/2}^{[0]} + \frac{2}{3}\phi_{1/2}^{[0]}\right) + \frac{1}{2}V_1\left(\hat{q}_1 - \frac{1}{3}\hat{q}_1^x\right). \tag{3.134}$$

The outer boundary cell $k = N$ gives us the asymptotic boundary condition. The cell-averaged current in the Nth cell is given by

$$r_N^2 J_N^{[1]} = -\frac{1}{\hat{\sigma}_{t,N}} \sum_{i=1}^{N} \frac{1}{\Delta x_{N,i-1/2}} \left(\psi_{N+1/2,i-1/2}^{+[0]} - \psi_{N-1/2,i-1/2}^{+[0]} \right.$$

$$\left. - \psi_{N-1/2,i-1/2}^{-[0]} + \psi_{N+1/2,i-1/2}^{-[0]} \right) w_{N,i-1/2}^y.$$

$$(3.135)$$

Substituting Eqs. (3.120), (3.121) into Eq. (3.135), we get

$$r_N^2 J_N^{[1]} = -\frac{1}{\hat{\sigma}_{t,N}} \left[\sum_{i=1}^{N} \frac{1}{\Delta x_{N,i-1/2}} \left(\psi_{N+1/2,i-1/2}^{+[0]} + \psi_{N+1/2,i-1/2}^{-[0]} \right) w_{N,i-1/2}^y \right.$$

$$\left. - \phi_{N-1/2}^{[0]} \sum_{i=1}^{N} \frac{w_{N,i-1/2}^y}{\Delta x_{N,i-1/2}} \right] = -\frac{1}{\hat{\sigma}_{t,N}} \left[\phi_{N+1/2}^{[0]} - \phi_{N-1/2}^{[0]} \right] \sum_{i=1}^{N} \frac{w_{N,i-1/2}^y}{\Delta x_{N,i-1/2}},$$

$$(3.136)$$

where

$$\phi_{N+1/2}^{[0]} = \left[\sum_{i=1}^{N} \frac{w_{N,i-1/2}^y}{\Delta x_{N,i-1/2}} \right]^{-1} \sum_{i=1}^{N} \frac{1}{\Delta x_{N,i-1/2}} \left(\psi_{N+1/2,i-1/2}^{+[0]} + \psi_{N+1/2,i-1/2}^{-[0]} \right) w_{N,i-1/2}^y.$$

$$(3.137)$$

Equation (3.137) leads to

$$\phi_{N+1/2}^{[0]} = \left[\sum_{i=1}^{N} \frac{w_{N,i-1/2}^y}{\Delta x_{N,i-1/2}} \right]^{-1} \sum_{i=1}^{N} \frac{1}{\Delta x_{N,i-1/2}} \left(\frac{1}{2} \phi_{N+1/2}^{[0]} + \psi_{i-1/2}^{in} \right) w_{N,i-1/2}^y. \qquad (3.138)$$

Thus, the asymptotic boundary condition of LLCM is defined as

$$\phi_{N+1/2}^{[0]} = \frac{2}{\left[\sum_{i=1}^{N} \frac{w_{N,i-1/2}^y}{\Delta x_{N,i-1/2}} \right]} \left(\sum_{i=1}^{N} \psi_{i-1/2}^{in} \frac{w_{N,i-1/2}^y}{\Delta x_{N,i-1/2}} \right). \qquad (3.139)$$

Note that the above analysis and results are similar to those of the moment-based linear characteristic method of tubes [23].

3.3 Explicit Slope Long Characteristic Method

In this section, we derive an explicit slope method of long characteristics (ESLC) for 1-D spherical geometry in (x, y) variables. This method approximates the scattering source term by means of a linear function, the slope of which is defined in terms of cell-averaged scalar flux [20]. This ultimately reduces the number of unknowns per cell.

Let us consider the following linear approximation of the scalar flux for $x_{k+1/2, i-1/2} \leq x \leq x_{k-1/2, i-1/2}$ ($\mu > 0$)

$$\phi_{k,i-1/2}(x) = \bar{\phi}_k + \frac{2}{\Delta x_{k,i-1/2}}(x - \bar{x}_{k,i-1/2})\hat{\phi}_k^+ . \tag{3.140}$$

Here $\hat{\phi}_k^+$ is the slope, defined such that

$$\phi_{k,i-1/2}(\bar{x}_{k,i-1/2}) = \bar{\phi}_k , \tag{3.141}$$

$$\phi_{k,i-1/2}(x_{k+1/2, i-1/2}) = \phi_{k+1/2} , \tag{3.142}$$

where the cell-edge value $\phi_{k+1/2}$ is determined by requiring the net current across cell boundaries to be continuous

$$J\big|_{r=r_{k+1/2}+0} = J\big|_{r=r_{k+1/2}-0} , \tag{3.143}$$

where the current is approximated by Fick's Law

$$J(r) = -\frac{1}{3\sigma_{t,k}}\frac{d\phi}{dr} . \tag{3.144}$$

Using finite difference to discretize the slope term,

$$-\frac{1}{3\sigma_{t,k}}\frac{\phi_{k+1/2} - \bar{\phi}_k}{2\Delta r_k} = -\frac{1}{3\sigma_{t,k+1}}\frac{\bar{\phi}_{k+1} - \phi_{k+1/2}}{2\Delta r_{k+1}} , \tag{3.145}$$

where

$$\Delta r_k = r_{k+1} - r_k \,. \tag{3.146}$$

Solving for $\phi_{k+1/2}$ we obtain

$$\hat{\phi}_k^+ = \frac{\xi_k(\bar{\phi}_{k+1} - \bar{\phi}_k)}{\xi_k + \xi_{k+1}} \,, \tag{3.147}$$

$$k = 1, ..., N - 1 \,,$$

$$\xi_k = \sigma_{t,k} \Delta r_k \,. \tag{3.148}$$

For $-x_{k+1/2, i-1/2} \leq x \leq -x_{k-1/2, i-1/2} \,(\mu < 0)$, we approximate the scalar flux as

$$\phi_{k,i-1/2}(x) = \bar{\phi}_k - \frac{2}{\Delta x_{k,i-1/2}}(x + \bar{x}_{k,i-1/2})\hat{\phi}_k^- \,, \tag{3.149}$$

where

$$\phi_{k,i-1/2}(-\bar{x}_{k,i-1/2}) = \bar{\phi}_k \,, \tag{3.150}$$

$$\phi_{k,i-1/2}(-x_{k-1/2,i-1/2}) = \phi_{k-1/2} \,. \tag{3.151}$$

As a result, we get

$$\hat{\phi}_k^- = \frac{\xi_k(\bar{\phi}_k - \bar{\phi}_{k-1})}{\xi_k + \xi_{k-1}} \,, \tag{3.152}$$

$$k = 2, ..., N \,.$$

For the Nth cell, $k = N$, we follow the requirement that the net current across cell boundaries must be continuous

$$J\big|_{r=r_{N+1/2}} = J\big|_{r=r_{N+1/2}-0} \,, \tag{3.153}$$

and therefore

$$J(r_{N+1/2}) = -\frac{1}{3\sigma_{t,k}}\frac{d\phi}{dr}\big|_{r=r_{N+1/2}-0} \,. \tag{3.154}$$

Using finite difference to discretize the slope term,

$$J(r_{N+1/2}) = -\frac{2}{3\sigma_{t,N}}\frac{\phi_{N+1/2} - \bar{\phi}_N}{\Delta r_N}. \tag{3.155}$$

The net current at the boundary is defined by means of the diffusion approximation

$$
\begin{aligned}
J(r_{N+1/2}) &= \int_{-1}^{1}\mu\psi(r_{N+1/2},\mu)d\mu = \int_{-1}^{0}\mu\psi(r_{N+1/2},\mu)d\mu + \int_{0}^{1}\mu\psi(r_{N+1/2},\mu)d\mu \\
&= J^{in} + \int_{0}^{1}\mu\left(\frac{1}{2}\tilde{\phi}_{N+1} + \frac{3}{2}\mu J(r_{N+1})\right)d\mu \\
&= J^{in} + \frac{1}{4}\phi_{N+1/2} + \frac{1}{2}J(r_{N+1}),
\end{aligned}
\tag{3.156}
$$

then

$$J(r_{N+1/2}) = 2J^{in} + \frac{1}{2}\phi_{N+1/2}, \tag{3.157}$$

where

$$J^{in} = \int_{-1}^{0}\mu\psi^{in}(\mu)d\mu. \tag{3.158}$$

By equating Eqs. (3.155) and (3.156) and utilizing Eq. (3.140), we get

$$\phi_N^+ = -\frac{3\xi_N}{(4+3\xi_N)}(4J^{in} + \bar{\phi}_N). \tag{3.159}$$

For the 1st cell, $k = 1$, the net current at the origin is zero, therefore

$$-\frac{1}{3\sigma_{t,k}}\frac{d\phi}{dr}\Big|_{r=0} = 0, \tag{3.160}$$

and therefore

$$\hat{\phi}_1^- = 0. \tag{3.161}$$

50

The resulting equations of ESLC method are the following:

$$\psi^-_{k-1/2,i-1/2} = \psi^-_{k+1/2,i-1/2} e^{-\tau_{k,i-1/2}} + \frac{1}{2\sigma_{t,k}}(1 - e^{-\tau_{k,i-1/2}})(\sigma_{t,k}\bar{\phi}_k + q_k)$$

$$- \frac{1}{\sigma_{t,k}\tau_{k,i-1/2}}\left[\frac{\tau_{k,i-1/2}}{2}(1 + e^{-\tau_{k,i-1/2}}) + e^{-\tau_{k,i-1/2}} - 1\right](\sigma_{t,k}\hat{\phi}^-_k + q^x_k),$$

$$(3.162)$$

$$\psi^-_{k-1/2,i-1/2} - \psi^-_{k+1/2,i-1/2} + \sigma_{t,k}\Delta x_{k,i-1/2}\psi^-_{k,i-1/2} = \frac{1}{2}(\sigma_{t,k}\bar{\phi}_k + q_k), \qquad (3.163)$$

$$\psi^-_{N+1/2,i-1/2} = \psi^{in}(y_{i-1/2}), \qquad (3.164)$$

$$k = N, ..., i,$$

$$\psi^+_{k+1/2,i-1/2} = \psi^+_{k-1/2,i-1/2} e^{-\sigma_{t,k}\Delta x_{k,i-1/2}} + \frac{1}{2\sigma_{t,k}}(1 - e^{-\tau_{k,i-1/2}})(\sigma_{t,k}\bar{\phi}_k + q_k)$$

$$+ \frac{1}{\sigma_{t,k}\tau_{k,i-1/2}}\left[\frac{\tau_{k,i-1/2}}{2}(1 + e^{-\tau_{k,i-1/2}}) + e^{-\tau_{k,i-1/2}} - 1\right](\sigma_{t,k}\hat{\phi}^+_k + q^x_k),$$

$$(3.165)$$

$$\psi^+_{k+1/2,i-1/2} - \psi^+_{k-1/2,i-1/2} + \sigma_{t,k}\Delta x_{k,i-1/2}\psi^+_{k,i-1/2} = \frac{1}{2}(\sigma_{t,k}\bar{\phi}_k + q_k), \qquad (3.166)$$

$$\psi^+_{i-1/2,i-1/2} = \psi^-_{i-1/2,i-1/2}, \qquad (3.167)$$

$$k = i, ..., N,$$

$$\text{for} \quad i = 1, ..., N + 1,$$

where

$$\bar{\phi}_k = \frac{1}{V_k}\sum_{i=1}^{k}(\psi^-_{k,i-1/2} + \psi^+_{k,i-1/2})\Delta x_{k,i-1/2}w^y_{k,i-1/2}. \qquad (3.168)$$

ESLC is defined by Eqs. (3.147), (3.152), (3.159), (3.161), and (3.162)-(3.168).

This method generates inaccurate solutions in some unresolved boundary layer problems at points where the material interface incurs a significant change in the scattering

ratio

$$c = \frac{\sigma_s}{\sigma_t} \, .$$

At these diffusive interfaces ESLC yields inaccurate estimates of the slope, which result in an unphysical solution behavior in the diffusive region of the problem. In an attempt to nullify this phenomenon, it is necessary to introduce a slope limiter [20]. Here, we set the slope of the scalar flux to zero across those interfaces where the ratio of c across the boundary is greater than δ_c (see Algorithm 1). This eliminates the influence of the interface slope term and improves the accuracy of the solution -without refinement of the spatial grid. Note, the use of a slope limiter has no effect on problems were there is no dramatic change in c.

Algorithm 1: Slope Limiter.

---

if $\frac{c_k}{c_{k+1}} > 1$ **then**

   if $\frac{c_k}{c_{k+1}} \geqslant \delta_c$ **then**

       $\phi_k^+ = 0\,, \quad \phi_{k+1}^- = 0$

   end

end

if $\frac{c_k}{c_{k+1}} < 1$ **then**

   if $\frac{c_{k+1}}{c_k} \geqslant \delta_c$ **then**

       $\phi_k^+ = 0\,, \quad \phi_{k+1}^- = 0$

   end

end

Chapter 4

METHODS OF SHORT

CHARACTERISTICS

In this chapter, we apply the ideas behind the derivation of CMLC to short characteristic methods. The primary difference being short characteristic methods require interpolation to determine the angular flux value at each vertex of a cell as opposed to the long characteristic method where the characteristic spans the entire problem domain without the use of interpolation.

4.1 Classical Method of Short Characteristics

In this section we present the classical method of short characteristics [5, 6, 7]. We introduce a spatial grid

$$\{r_{j+1/2}, j = 1, ..., N, \ r_{1/2} = 0, \ r_{N+1/2} = R\}, \tag{4.1}$$

54

and angular mesh

$$\{\mu_{m+1/2}, m = 0, ..., M, \ \mu_{1/2} = -1, \ \mu_{M+1/2} = 1, \ \mu_{\frac{M-1}{2}+1} = 0\}, \tag{4.2}$$

(see Figure 4.1). For non-positive directions ($\mu_{m+1/2} \leq 0$), the angular flux at $(r_{j-1/2}, \mu_{m+1/2})$

vertex is determined as

$$\psi_{m+1/2,j-1/2} = \psi_{m,j}^* e^{-\sigma_{t,j}\Delta s_{m,j}} + \frac{1}{2\sigma_{t,j}}(\sigma_{s,j}\phi_j + q_j)(1 - e^{-\sigma_{t,j}\Delta s_{m,j}}), \quad j = N, ..., 1, \tag{4.3}$$

where $\psi_{m,j}^* = \psi(r_{j+1/2}, \mu_{m,j}^*)$ is the angular flux at the incoming edge of (m,j)-cell at

$r = r_{j+1/2}$ and

$$\mu = \mu_{m,j}^* = -\sqrt{1 - \frac{r_{j-1/2}}{r_{j+1/2}}(1 - \mu_{m+1/2}^2)}. \tag{4.4}$$

The value of $\psi_{m,j}^*$ is obtained, for example, by linear interpolation with respect to μ between

the known vertex-values of the angular flux closest to $\mu_{m,j}^*$ (yellow vertices). The particle

track length in the cell is given by

$$\Delta s_{m,j} = r_{j-1/2}\mu_{m+1/2} - r_{j+1/2}\mu_{m,j}^*. \tag{4.5}$$

For positive directions ($\mu_{m'+1/2} > 0$) in (m', j)-cell, we have

$$\psi_{m'+1/2,j+1/2} = \psi_{m',j}^* e^{-\sigma_{t,j}\Delta s_{m',j}} + \frac{1}{2\sigma_{t,j}}(\sigma_{s,j}\phi_j + q_j)(1 - e^{-\sigma_{t,j}\Delta s_{m',j}}), \quad j = 1, ..., N, \tag{4.6}$$

where $\psi_{m',j}^* = \psi(r_{j-1/2}, \mu_{m',j}^*)$ is the angular flux at incoming edge of (m', j)-cell at $r = r_{j-1/2}$ and

$$\mu = \mu_{m',j}^* = \sqrt{1 - \frac{r_{j+1/2}}{r_{j-1/2}}(1 - \mu_{m'+1/2}^2)}. \tag{4.7}$$

The track length is

$$\Delta s_{m',j} = r_{j+1/2}\mu_{m'+1/2} - r_{j-1/2}\mu_{m',j}^*. \tag{4.8}$$

The cell-average scalar flux ϕ_j is determined by means of cell-edge scalar fluxes

$$\phi_{j-1/2} = \sum_{m=0}^{M} \psi_{m+1/2,j-1/2} w_m \, .$$

.

4.2   Formulation of a Locally Conservative Method of Short Characteristics

In this section we formulate a locally conservative method of short characteristics (LCMSC) based on the classical method of short characteristics presented above. Figure 4.1 shows the particle paths (tracks) inside each cell in case of (r, μ) coordinates. The interpretation of the method of short characteristics in (x, y) coordinated is presented in Figure 4.2. Based on this viewpoint, we define the track-average value of the angular flux in the following form:

$$\psi_{m,j} = (1 - \alpha_{m,j}) \psi_{m+1/2,j-1/2} + \alpha_{m,j} \psi_{m,j}^* \quad \text{for } \mu_{m+1/2} \le 0 \, , \tag{4.9}$$

$$\alpha_{m,j} = \frac{1}{\sigma_{t,j} \Delta s_{m,j}} - \frac{e^{-\sigma_{t,j} \Delta s_{m,j}}}{1 - e^{-\sigma_{t,j} \Delta s_{m,j}}} \, , \tag{4.10}$$

$$\psi_{m',j} = (1 - \alpha_{m',j}) \psi_{m'+1/2,j+1/2} + \alpha_{m',j} \psi_{m',j}^* \quad \text{for } \mu_{m'+1/2} \, 0 \, . \tag{4.11}$$

As a result the detailed balance equation for each track in case $\mu_{m+1/2} \le 0$ can be formulated as follows:

$$\psi_{m+1/2,j-1/2} - \psi_{m,j}^* + \sigma_{t,j} \Delta s_{m,j} \psi_{m,j} = \frac{\Delta s_{m,j}}{2} (\sigma_{s,j} \phi_j + q_j) \, . \tag{4.12}$$

The value of y-coordinate for the track in (m, j) cell is given by

$$y = \tilde{y}_{m,j} = r_{j-1/2} \sqrt{1 - \mu_{m+1/2}^2} \, . \tag{4.13}$$

In case $\mu_{m'+1/2} > 0$ we have

$$\psi_{m'+1/2,j+1/2} - \psi^*_{m',j} + \sigma_{t,j}\Delta s_{m',j}\psi_{m',j} = \frac{\Delta s_{m',j}}{2}\left(\sigma_{s,j}\phi_j + q_j\right),\tag{4.14}$$

$$\tilde{y}_{m',j} = r_{j+1/2}\sqrt{1 - \mu^2_{m'+1/2}}\,.\tag{4.15}$$

To define the cell-average scalar flux, we formulate the balance equation in the jth spatial interval similar to Eq. (3.17) and integrate numerically the track-average angular fluxes with respect to y in each cell that belongs to the jth spatial interval (see Figure 4.2). As a result, we have

$$\phi_j = \frac{1}{V_j}\left[\sum_{m=0}^{\frac{M-1}{2}}\psi_{m,j}\Delta s_{m,j}\tilde{w}^y_{m,j} + \sum_{m'=\frac{M-1}{2}+2}^{M}\psi_{m',j}\Delta s_{m',j}\tilde{w}^y_{m',j}\right],\tag{4.16}$$

$$V_j = \frac{1}{2}\left(\sum_{m=0}^{\frac{M-1}{2}}\Delta s_{m,j}\tilde{w}^y_{m,j} + \sum_{m'=\frac{M-1}{2}+2}^{M}\Delta s_{m',j}\tilde{w}^y_{m',j}\right),\tag{4.17}$$

where $\tilde{w}^y_{m,j}$ are corresponding quadrature weights

$$\tilde{w}^y_{0,j} = \frac{1}{4}\left(\tilde{y}^2_{1,j} - \tilde{y}^2_{0,j}\right),\tag{4.18}$$

$$\tilde{w}^y_{m,j} = \frac{1}{4}\left(\tilde{y}^2_{m+1,j} - \tilde{y}^2_{m-1,j}\right),\ m = 1,...,\frac{M-1}{2},\frac{M-1}{2}+2,...,M-1\,,$$

$$\tilde{w}^y_{M,j} = \frac{1}{4}\left(\tilde{y}^2_{M,j} - \tilde{y}^2_{M-1,j}\right).\tag{4.19}$$

Note that $\Delta s_{\frac{M-1}{2}+1,j} = 0$.

Figure 4.1: The method of short characteristics in (r, μ) coordinates.
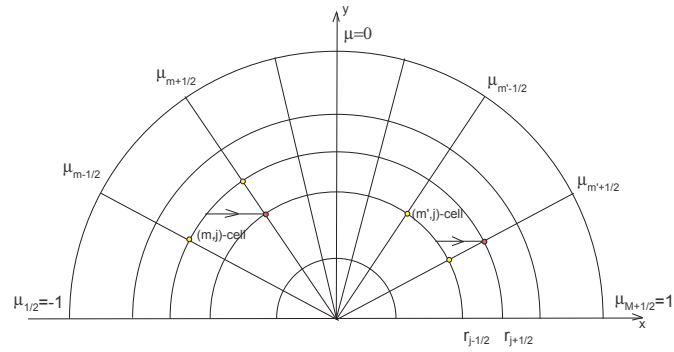
Figure 4.2: The method of short characteristics in (x, y) coordinates.
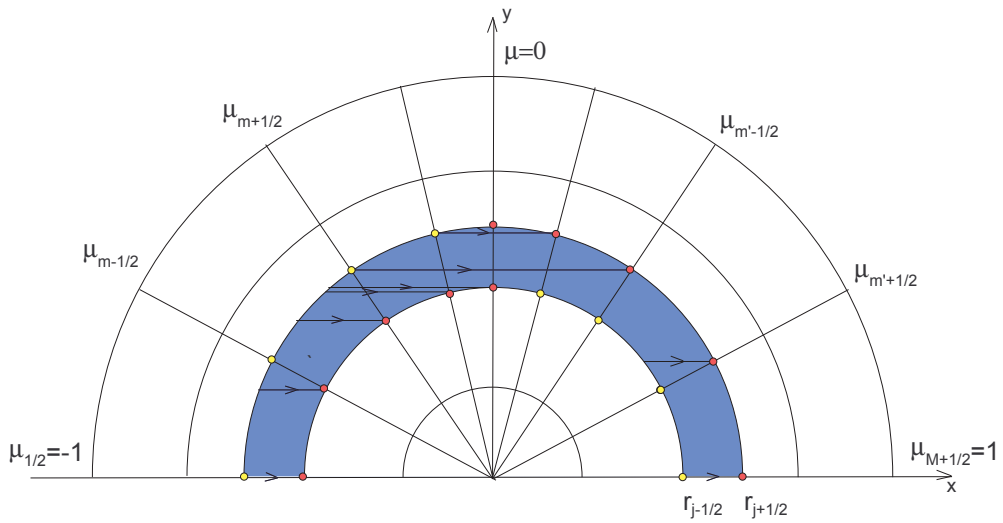
Figure 4.3: Tracks of characteristics for calculating the cell-average scalar flux in LCMSC.

Figure 4.3 demonstrates the resulting set of tracks that are used by LCMSC in the jth spatial interval to calculate the angular fluxes in vertices and as a result track-average angular fluxes which then defines the way the spatially averaged scalar flux is computed. We notice that the sets of tracks for $\mu < 0$ and $\mu > 0$ are not symmetric having different track lengths and value of y-coordinates, namely

$$\Delta s_{m',j} \neq \Delta s_{m,j}, \quad \tilde{y}_{m',j} \neq \tilde{y}_{m,j} \quad \text{for } \mu_{m'+1/2} = |\mu_{m+1/2}|. \tag{4.20}$$

This leads, for example, to the fact that the quadratures weights for scalar flux calculation are different for positive and negative directions. It is possible to reformulate the proposed method to get desired symmetry.

4.3 Formulation of a Symmetrized Locally Conservative Method of Short Characteristics

In this section we propose a symmetrized locally conservative method of short characteristics (SLCMSC) based on the conservative method of short characteristics presented above. The formulation of SLCMSC for the non-positive directions $(\mu_{m+1/2} \leq 0)$ is identical to one of LCMSC. Hence, we consider a characteristic that passes through the vertex $(r_{j-1/2}, \mu_{m+1/2},)$, where the unknown angular flux, $(\psi_{m+1/2,j-1/2})$, is to be determined (see Figures 4.4 and 4.5). Then, one needs to calculate the value of $\psi_{m,j}^* = \psi(r_{j+1/2}, \mu_{m,j}^*)$ at the location where the given characteristics intersect with the cell face at $r = r_{j+1/2}$. Thus, SLCMSC performs "upstream" interpolation for $\mu_{m+1/2} \leq 0$.
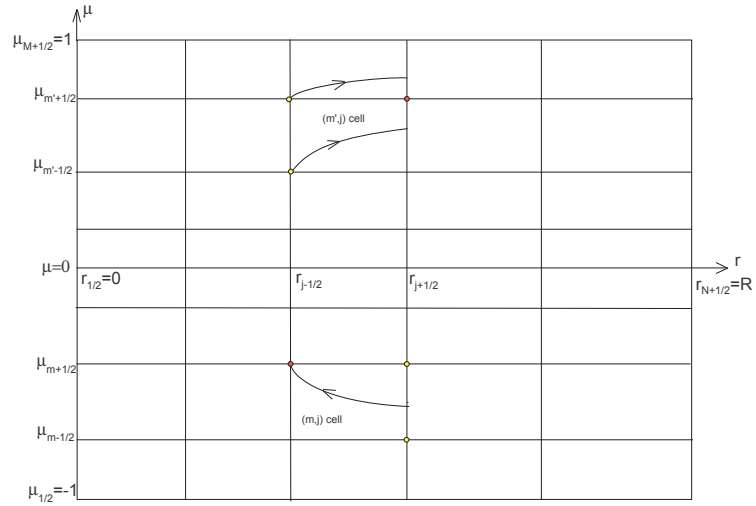
Figure 4.4: The symmetrized locally conservative method of short characteristics in (r, μ) coordinates.
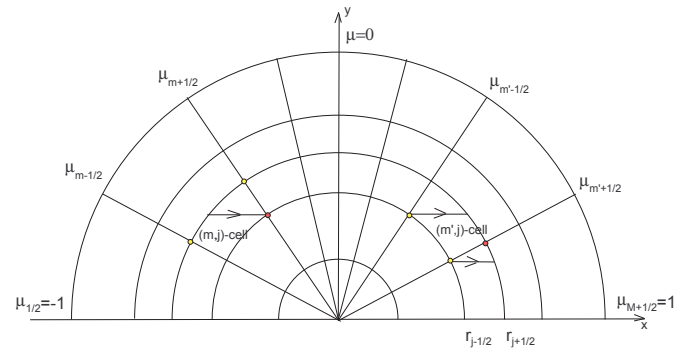

Figure 4.5: The symmetrized locally conservative method of short characteristics in (x, y) coordinates.
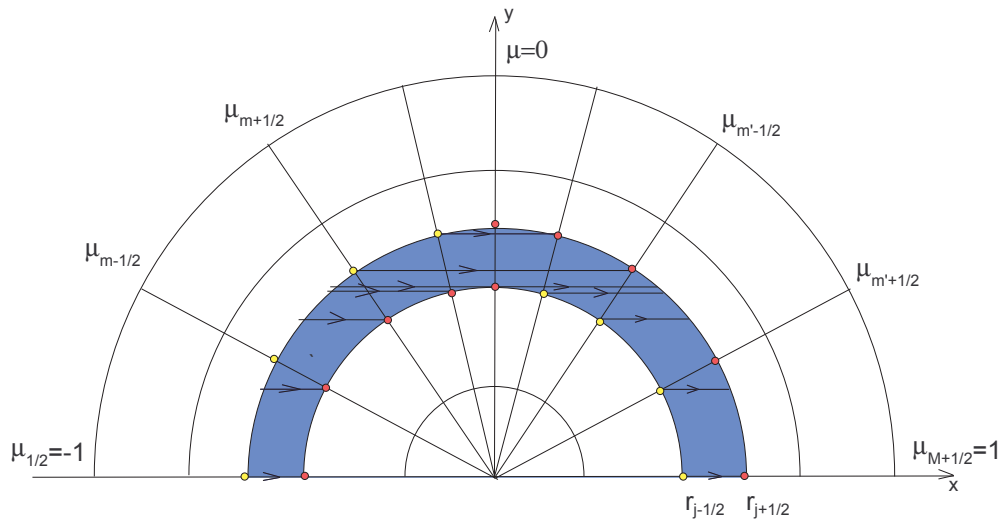

Figure 4.6: Tracks of characteristics for calculating the cell-average scalar flux in SLCMSC.

In case $\mu_{m'+1/2} > 0$, the proposed method uses "downstream" interpolations. We use only characteristics that originate at upstream vertices $(r_{j-1/2}, \mu_{m'-1/2},)$, where the solution is known. First, the transport equation is solved along each of these characteristics:

$$\psi^\circ_{m',j} - \psi_{m'-1/2,j-1/2} + \sigma_{t,j}\Delta s_{m',j}\psi_{m',j} = \frac{\Delta s_{m',j}}{2}(\sigma_{s,j}\phi_j + q_j),$$

(4.21)

$$\psi_{m',j} = (1 - \alpha_{m',j})\psi^\circ_{m',j} + \alpha_{m',j}\psi_{m'-1/2,j-1/2},$$

(4.22)

$$\tilde{y}_{m',j} = r_{j-1/2}\sqrt{1 - \mu^2_{m'-1/2}}.$$

(4.23)

to determine $\psi^\circ_{m',j}$ at a position where the given characteristic intersects the downstream face at $r = r_{j+1/2}$ (see Figures 4.4 and 4.5). Then, these values of angular fluxes are used to calculate the angular fluxes at location of downstream vertices.

The cell-average scalar flux is defined as follows

$$\phi_j = \frac{1}{V_j}\left[\sum_{m:\mu\leq0} \psi_{m,j}\Delta s_{m,j}\tilde{w}^y_{m,j} + \sum_{m':\mu>0} \psi_{m',j}\Delta s_{m',j}\tilde{w}^y_{m',j}\right],$$

(4.24)

$$V_j = \frac{1}{2}\left[\sum_{m:\mu\leq0} \Delta s_{m,j}\tilde{w}^y_{m,j} + \sum_{m':\mu>0} \Delta s_{m',j}\tilde{w}^y_{m',j}\right],$$

(4.25)

where $\tilde{w}^y_{m,j}$ are corresponding quadrature weights for integration over y defined by $\tilde{y}_{m,j}$. Note that the discretized net leakage rate is given by

$$T_j = \sum_{m:\mu\leq0} (\psi_{m+1/2,j-1/2} - \psi^*_{m,j})\tilde{w}^y_{m,j} + \sum_{m':\mu>0} (\psi^\circ_{m',j} - \psi_{m'-1/2,j-1/2})\tilde{w}^y_{m',j}.$$

(4.26)

4.4 Asymptotic Diffusion Analysis of SLCMSC

The asymptotic diffusion analysis of SLCMSC in the interior of an optically thick diffusion domain shows that the leading-order solution satisfies the following equations:

$$\sum_{m:\mu\leq 0}(\psi^{[0]}_{m+1/2,j-1/2}-\psi^{*[0]}_{m,j})\tilde{w}^y_{m,j}+\sum_{m':\mu>0}(\psi^{\circ[0]}_{m',j}-\psi^{[0]}_{m'-1/2,j-1/2})\tilde{w}^y_{m',j}=0\,. \tag{4.27}$$

$$\psi^{[0]}_{m+1/2,j-1/2}=\frac{1}{2}\phi^{[0]}_j\,,\quad m:\ \mu\leq 0\,, \tag{4.28}$$

$$\psi^{[0]}_{m'-1/2,j+1/2}=\frac{1}{2}\phi^{[0]}_j\quad m':\ \mu\leq 0. \tag{4.29}$$

Hence the leading-order scalar flux of SLCMSC satisfies the following equation in interior cells:

$$\left(\phi^{[0]}_j-\phi^{[0]}_{j+1}\right)-\left(\phi^{[0]}_{j-1}-\phi^{[0]}_j\right)=0\,,\quad j=1,...,N-1\,. \tag{4.30}$$

The SLCMSC asymptotic boundary condition is defined as

$$\phi^{[0]}_{N+1}=\frac{2}{\tilde{F}}\sum_{m:\mu\leq 0}\psi^{in}(\mu^*_{m,N})\tilde{w}^y_{m,N}\,,\quad \tilde{F}=\sum_{m:\mu\leq 0}\tilde{w}^y_{m,N}\,. \tag{4.31}$$

The results of analysis of SLCMSC are similar to those of CMLC in that the total source term does not influence the leading order solution in the thick diffusive limit and therefore does not limit to an accurate discretization of the diffusion equation.

Chapter 5

NUMERICAL RESULTS

5.1   Reed's Test

Problem 1. We present the results of the 1-D spherical geometry version of Reed's test problem [9]. First developed to illustrate the weaknesses of the diamond difference scheme, this test consists of multiple spatial regions with varying material characteristics that help determine a method's general performance and implementation. Reed's test does not address diffusive regions where spatial intervals have a large optical thickness. The definition of this test is shown in Table 5.1. Reed's test for 1-D spherical geometry, like the slab geometry version, is comprised of 40 equally spaced spatial intervals with the angular meshes for LCMSC and SLCMSC having 8 equal intervals. In this and other tests, we use linear interpolation in LCMSC and SLCMSC. Figure 5.1 shows cell-average scalar flux versus position for CMLC, LLCM, ESLC, LCSCM, and SLCMSC methods, cell-edge scalar fluxes for VMOC-LI and VMOC-PI, as well as the reference solution generated using CMLC

Region	Spatial Interval	σ_t	σ_s	q
1	$0 < r < 2$	50	0	50
2	$2 < r < 3$	5	0	0
3	$3 < r < 5$	0	0	0
4	$5 < r < 6$	1	0.9	0.7
5	$6 < r < 8$	1	0.9	0

on a very fine mesh with 1600 intervals.

These results demonstrate that most of the considered methods perform reasonably well for this heterogeneous problem. However, we note that LCMSC underestimates the solution in the domains influenced by the external source in non-optically thick scattering regions. A possible reason for such behavior could be the quality of numerical integration of the angular flux with respect to y based on a non-symmetric grid to generate the scalar flux. It is also possible that the resulting y-grid in case of LCMSC is not fine enough for positive directions.
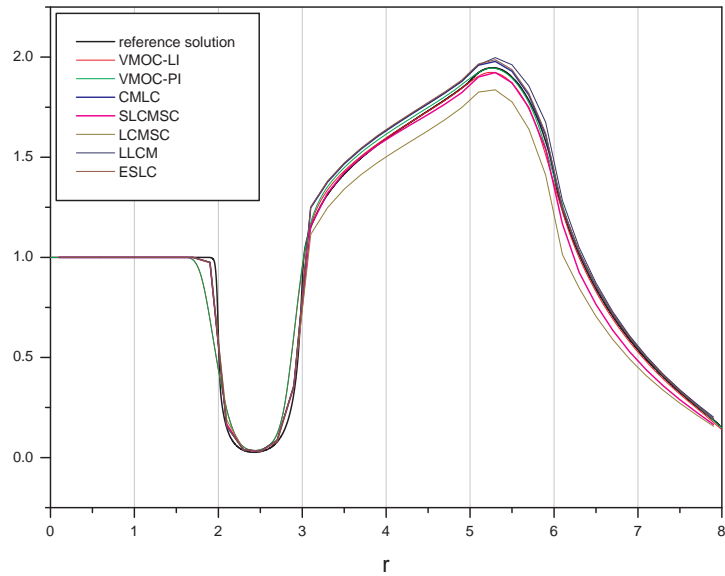
Figure 5.1: Problem 1. The scalar flux.

5.2 A Diffusion Test

Problem 2. We consider a sphere ($R = 11$) with two regions [15]. The central region with a source (Region 1) is surrounded by an optically thick, pure scattering region (Region 2). The cross sections for each subregion are given in Table 5.2. The boundary condition is vacuum. The spatial mesh is uniform and has 20 cells. The angular mesh for LCMSC and SLCMSC is the same as in Problem 1. The reference solution in Region 1 is constant and

$$\phi(r) = \frac{q}{\sigma_a} = 1 \,. \tag{5.1}$$

In the interior of Region 2, the transport solution is close to the solution of the diffusion equation with corresponding Dirichlet boundary conditions at r=10 and r=20 that has a form dependent on the numerical solution, $\phi(10)$:

$$\phi(r) = 20\phi(10)(\frac{1}{r} - \frac{1}{20}) \,. \tag{5.2}$$

Table 5.2: Test Problem 2

Region	Spatial Interval	σ_t	σ_s	q
1	$0 < r < 10$	100	90	10
2	$10 < r < 20$	100	100	0

The results are presented in Figures 5.2-5.13. We note that the numerical solutions of VMOC-LI and VMOC-PI have wrong shapes in Region 2. The VMOC-PI method generates the solution that has wrong sign of the second derivative of the solution and as a result it is convex (see Figures 5.3 and 5.4). Figures 5.5, 5.6, 5.7, 5.8, and 5.13 show solutions of CMLC, LLCM, ESLC, LCMSC, and SLCMSC and corresponding diffusion solutions. These methods generate numerical solutions with correct shape.
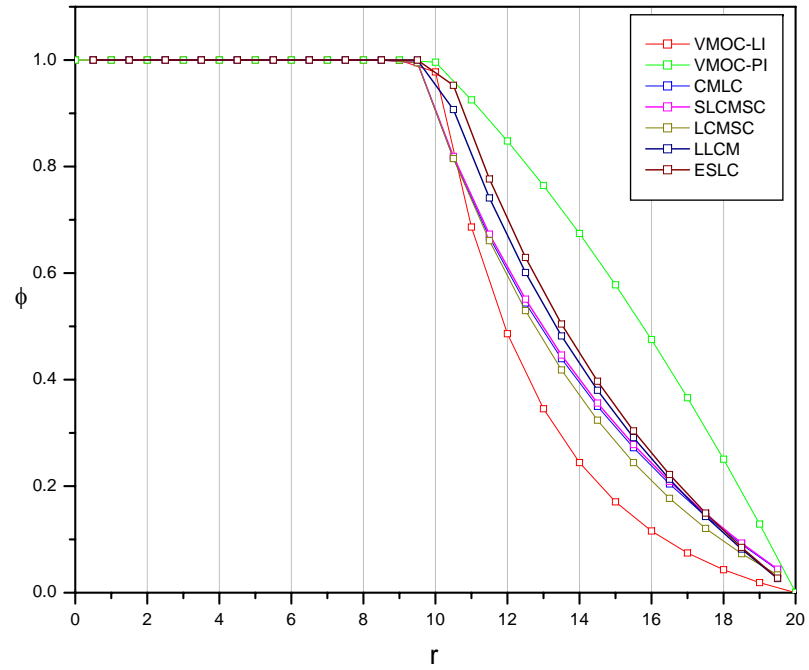
Figure 5.2: Problem 2. The scalar flux.
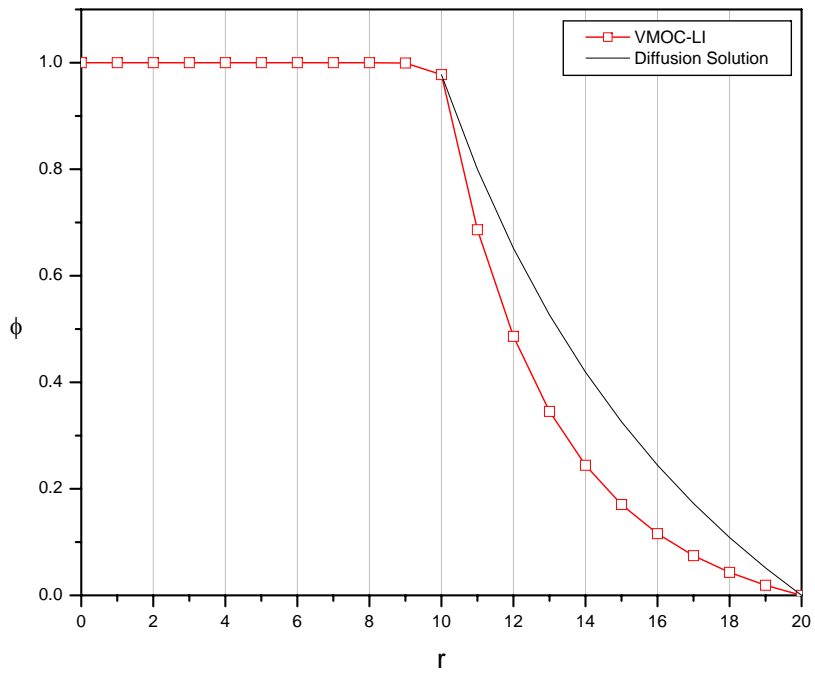
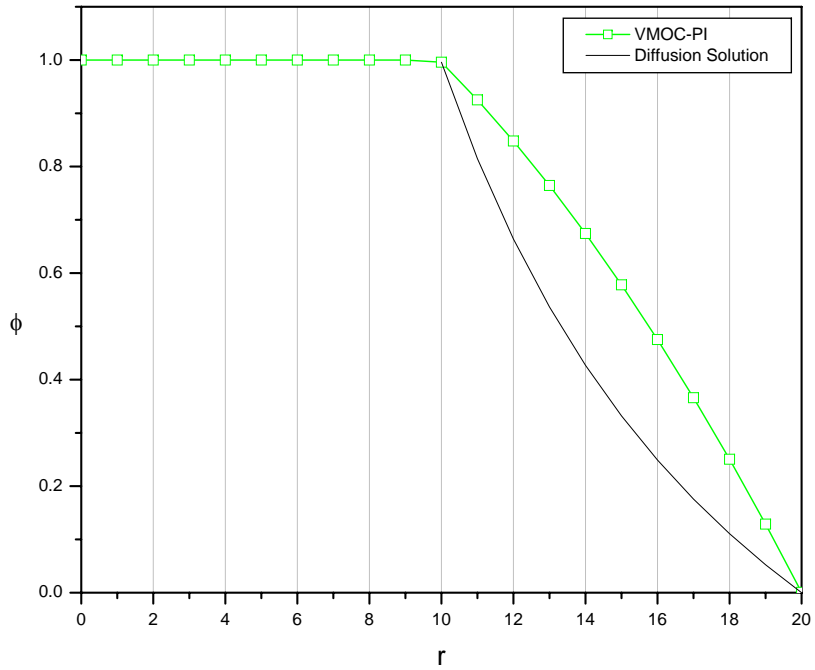Figure 5.3: Problem 2. The cell-edge scalar flux for VMOC-LI.

66

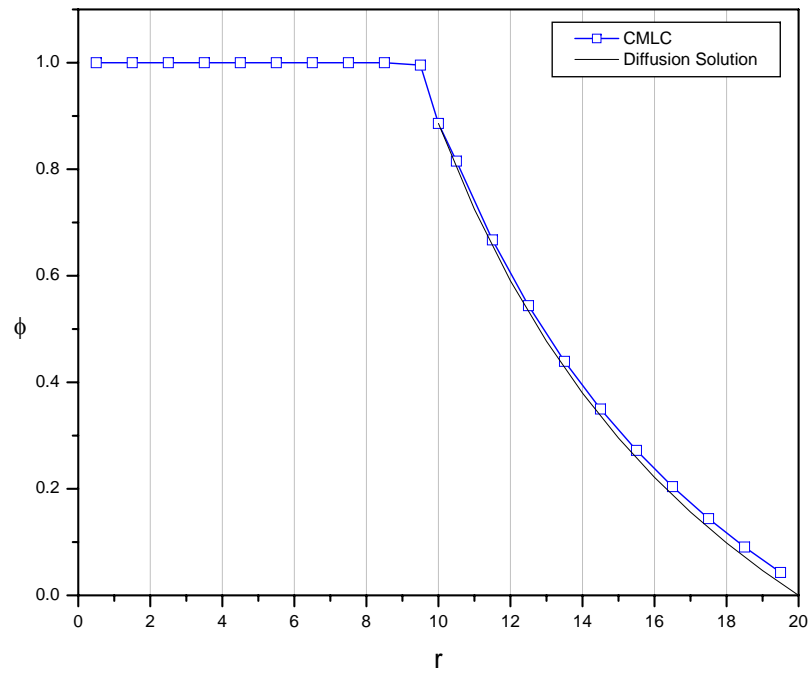Figure 5.4: Problem 2. The cell-edge scalar flux for VMOC-PI.

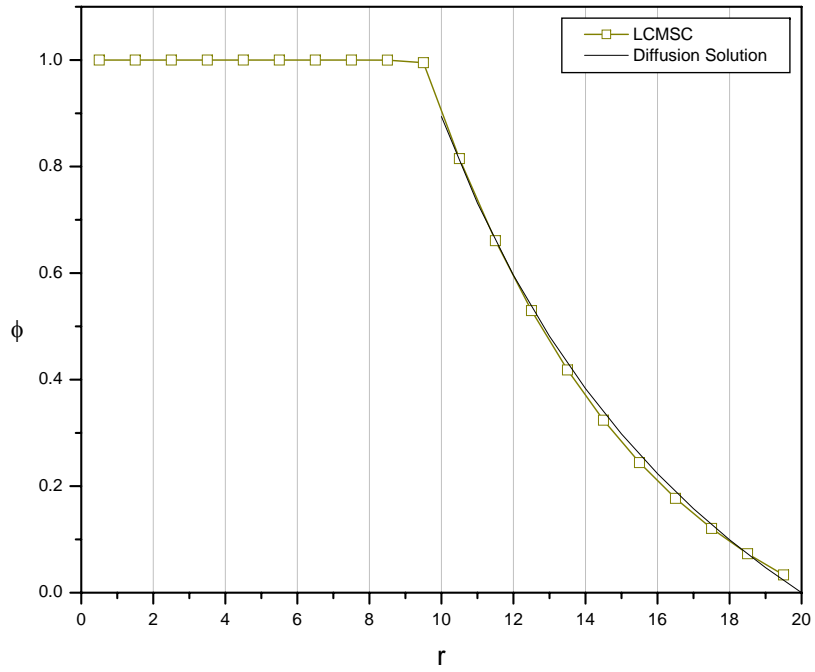Figure 5.5: Problem 2. The cell-average scalar flux for CMLC.

67

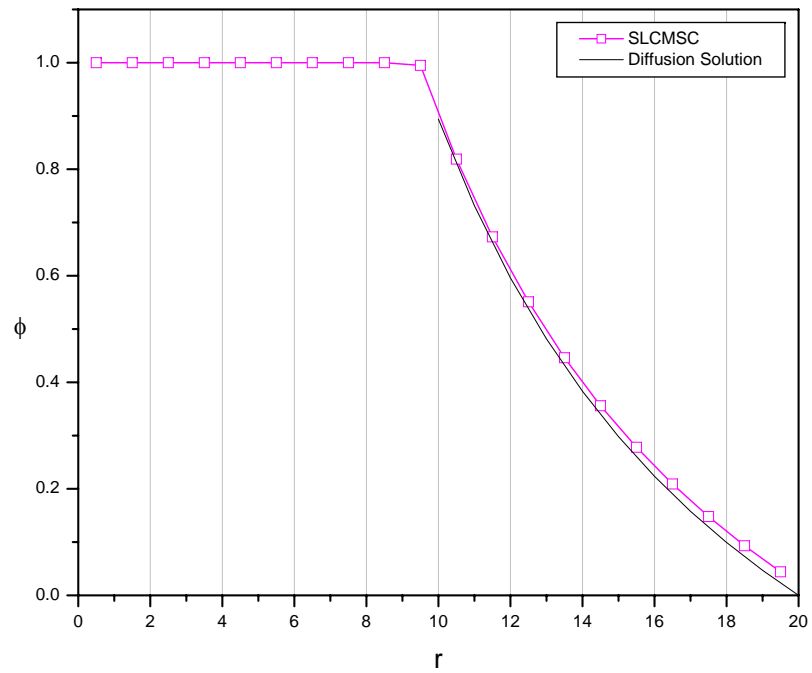Figure 5.6: Problem 2. The cell-average scalar flux for LCMSC.

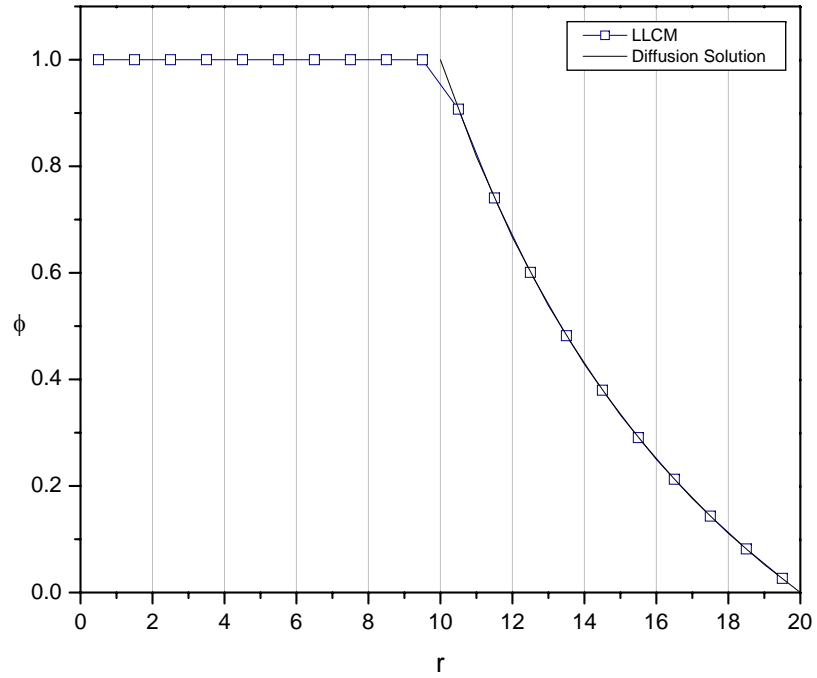Figure 5.7: Problem 2. The cell-average scalar flux for SLCMSC.

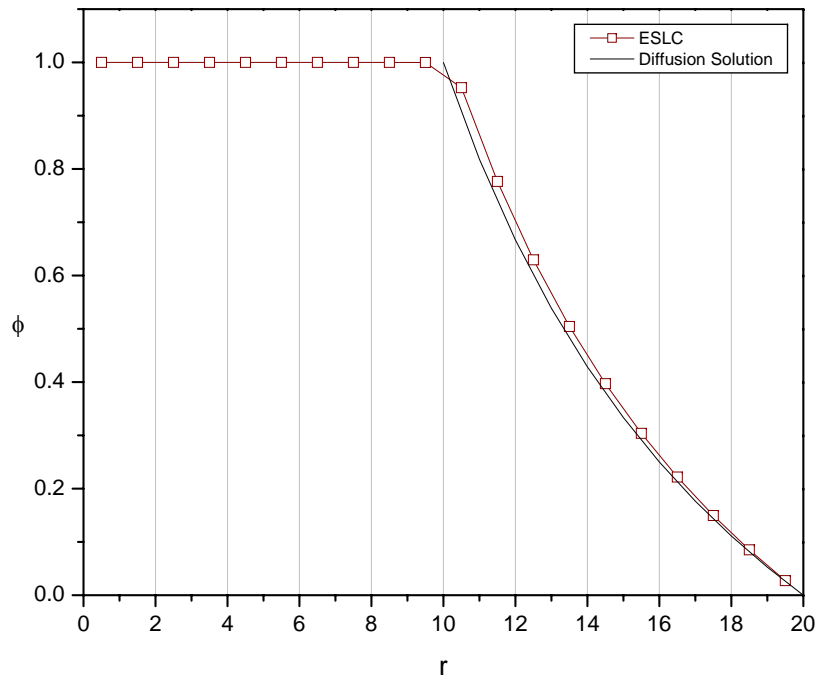Figure 5.8: Problem 2. The cell-average scalar flux for LLCM.

Figure 5.9: Problem 2. The cell-average scalar flux for ESLC.

5.3 A Test with an Unresolved Boundary Layer in a Diffusive Region

Problem 3. This problem is designed to test a method's ability to accurately reproduce the interior solution of a diffusive problem with an unresolved boundary layer. Due to the nature of radiative transfer problems, many of them are optically thick with cross sections around 10^6 making it impractical to refine the spatial grid for the purpose of resolving the diffusive boundary layer. The boundary conditions derived in an asymptotic analysis correspond to a method's ability to accurately reproduce this solution. We consider a source-free sphere ($R = 11$) with two regions (See Table 5.3): (i) pure scattering, central subregion (Region 1) with $\sigma_t=\sigma_s=100$, (ii) pure absorbing subregion (Region 2) with $\sigma_t=2$ [15]. There is an isotropic incident angular flux $\psi(r = 11, \mu < 0)=1$ on the boundary. A spatial mesh has 10 uniform cells in each region. The angular mesh for LCMSC and SLCMSC is the same as in Problem 1. The results are presented in Figures 5.10 - 5.15.

Table 5.3: Test Problem 3

Region	Spatial Interval	σ_t	σ_s	q
1	$0 < r < 10$	100	100	0
2	$10 < r < 11$	2	0	0

Table 5.4: Test Problem 4

Region	Spatial Interval	σ_t	σ_s	q
1	$0 < r < 10$	100	100	0
2	$10 < r < 11$	4	0	0

There exists an unresolved boundary layer at the interface between the two sub-regions (r=10). The flux incident on the sphere (at r=11) is attenuated in the outer pure absorbing region to create an anisotropic angular flux coming into the central diffusion region (at r=10). This incoming angular flux has the following form:

$$\psi(10,\mu) = e^{-\sigma_a(10\mu + \sqrt{11^2 - 10^2(1-\mu^2)})} \quad \mu < 0\,, \tag{5.3}$$

where $\sigma_a = \sigma_t - \sigma_s$.

The transport solution in the central domain asymptotically approaches the value of the scalar flux resulted from the asymptotic diffusion boundary condition at r=10 formed by the anisotropic angular flux (Eq.(5.3)) entering from the pure absorbing subregion. Analytic calculations show that the exact value is 0.14674. The results for VMOC-LI and VMOC-PI asymptotic analysis showed that these methods would perform poorly in the thick diffusion limit with the same predicted value (0.073831). Note the boundary condition was determined to be the same for both cases. This result is confirmed by the numerical values (Figure 5.10) of 0.073840 and 0.073844 for VMOC-LI and VMOC-PI, respectively. The solution of each case has relative error of 50%.

Now, we consider the new long and short characteristic methods developed in this thesis. The asymptotic analysis predicted that CMLC and SLCMSC give 0.14634 and 0.13809, correspondingly. The obtained numerical results of CMLC (0.14634) (Figure 5.11) and SLCMSC (0.13809) (Figure 5.12) confirm the theoretical prediction (Eqs. (3.62) and (3.67)) of the asymptotic analysis. Note that in this test the relative error of CMLC in the diffusion region is very small. It is about 0.27%. In the given problem CMLC generates the boundary condition with rather small relative error. In an equivalent 1D slab geometry

71

problem, the step characteristic (SC) method produces the solution with the relative error about 10%. These results enable us to see a distinction in performance between this SC-like method in spherical geometry and SC method in slab geometry. Note that the asymptotic boundary conditions of these two methods differ by the way the numerical integration is carried out and by the underlying phase-space grid. The relative error of SLCMSC solution is 5.9%. This shows the effect of differences between SLCMSC and CMLC in phase space grids and space-angle discretization as well as interpolation involved in SLCMSC. Let us modify this problem by increasing the absorption ($\sigma_a = 4$) in Region 2 (see Table 5.4). In this case, the analytic solution of the diffusion problem with asymptotic boundary condition in Region 1 has the value of 0.013989. Figure 5.15 demonstrates the CMLC solution of this problem. The relative error is now about 3.5%.

For the LCMSC case, the numerical results of 0.13471 (figure 5.12) show how the behavior for this diffusive problem differs for downstream versus upstream interpolation for $\mu > 0$ with a relative difference of 2% between SLCMSC and LCMSC. The relative error of the LCMSC solution is 8.2%.

Lastly, the ESLC method was not analyzed but was implemented and the numerical results are shown in Figures 5.13 and 5.14, ESLC and ESLC-SL. It was mentioned that ESLC fails to reproduce an accurate solution for some unresolved boundary layer problems. The numerical results for ESLC (4.2113) show this loss of accuracy. With the addition of a slope limiter, the numerical results for ESLC-SL (0.14581) showed a significant increase in accuracy with a relative error of 0.63% to the exact value.
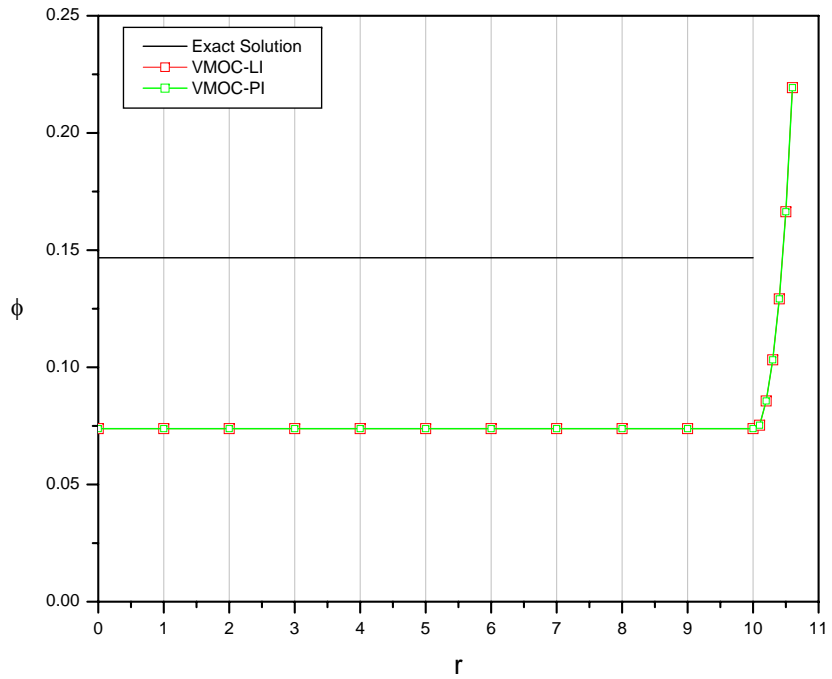
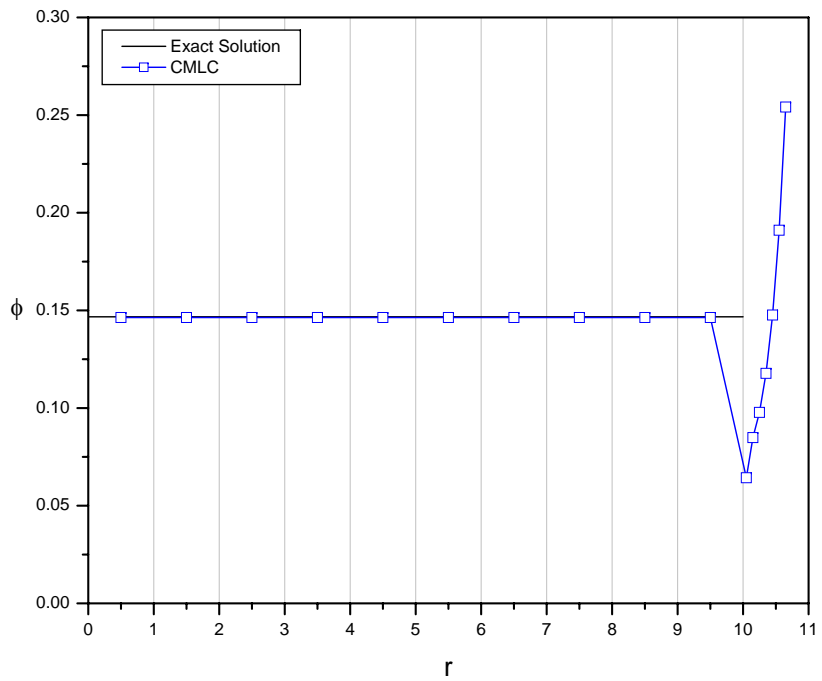Figure 5.10: Problem 3. The cell-edge scalar flux for VMOC-LI and VMOC-PI.

Figure 5.11: Problem 3. The cell-average scalar flux for CMLC.
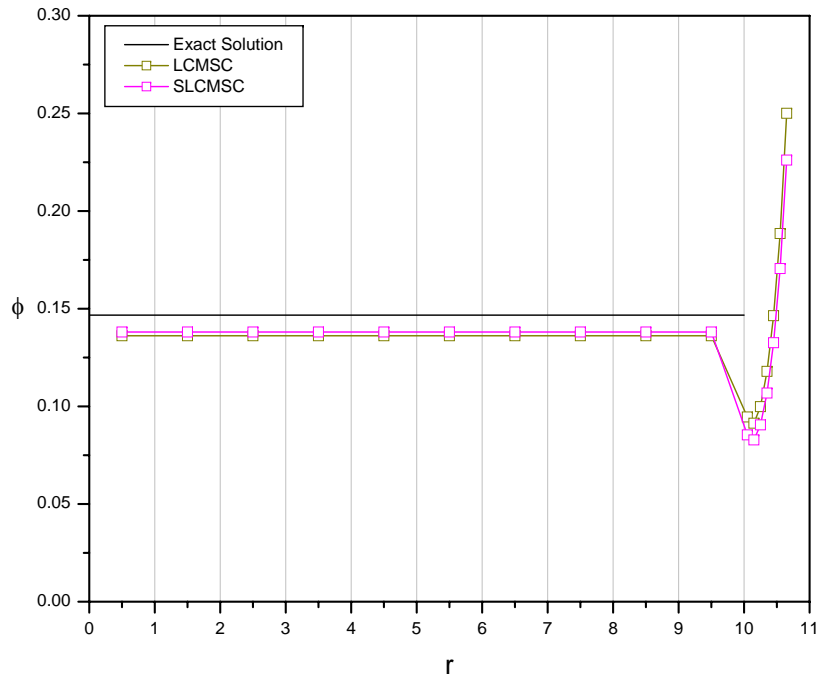
73

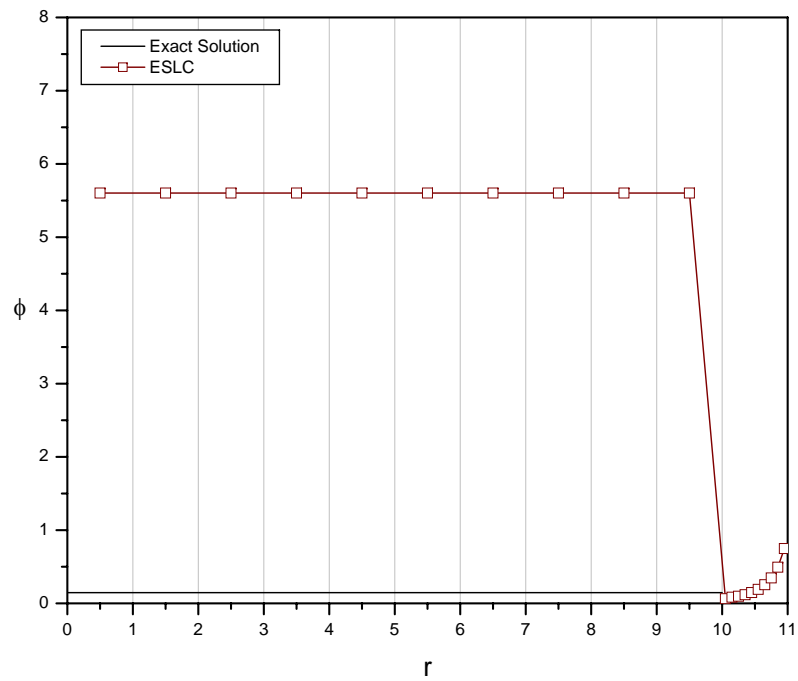Figure 5.12: Problem 3. The cell-average scalar flux for LCMSC and SLCMSC.

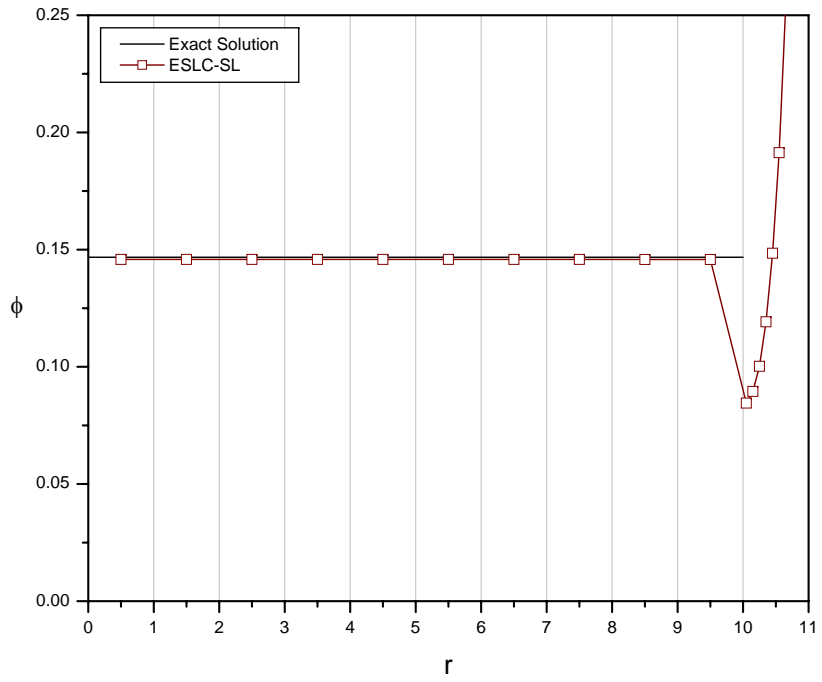Figure 5.13: Problem 3. The cell-average scalar flux for ESLC without slope limiter.

74

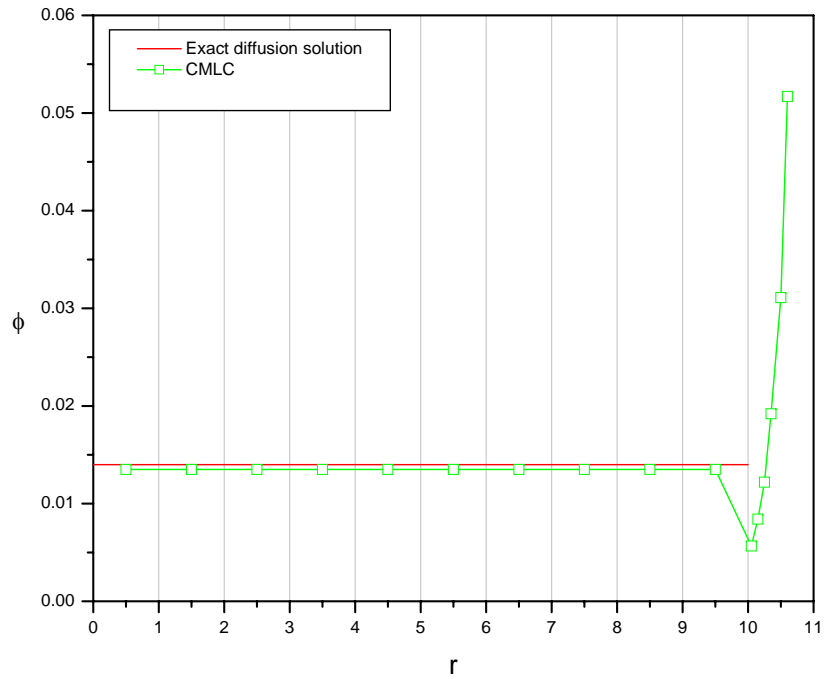Figure 5.14: Problem 3. The cell-average scalar flux for ESLC with slope limiter.

Figure 5.15: Problem 4. The cell-average scalar flux for CMLC.

75

5.4 Diffusion Limit Tests

Problem 5. We consider a homogeneous sphere $(R = 10)$ with $\sigma_t = \frac{1}{\varepsilon}$, $\sigma_a = \varepsilon$, and $q = \varepsilon$ [18]. Boundary condition is vacuum. A spatial mesh consists of 10 uniform intervals. Figures 5.16, 5.17, 5.18, 5.19, and 5.20 present the scalar flux versus position calculated by CMLC, LCMSC, SLCMSC, LLCM, and ESLC. As the value of ε in these tests decreases, the problem becomes more and more diffusive. The obtained amplitude of numerical solutions for CMLC, LCMSC, and SLCMSC decreases as ε decreases. This fact confirms the results of theoretical analysis of the methods under study. They do not lead to a good approximation of the diffusion equation in the asymptotic diffusion limit. Conversely, if we consider LLCM and ESLC, the numerical solutions demonstrate that the discretized transport solution limits to the discretized diffusion solution as ε decreases.
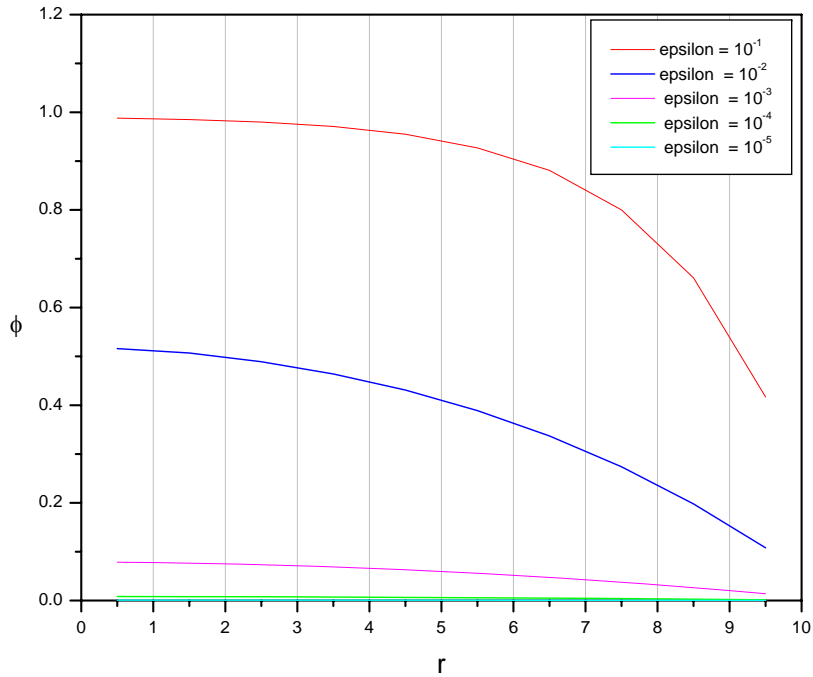

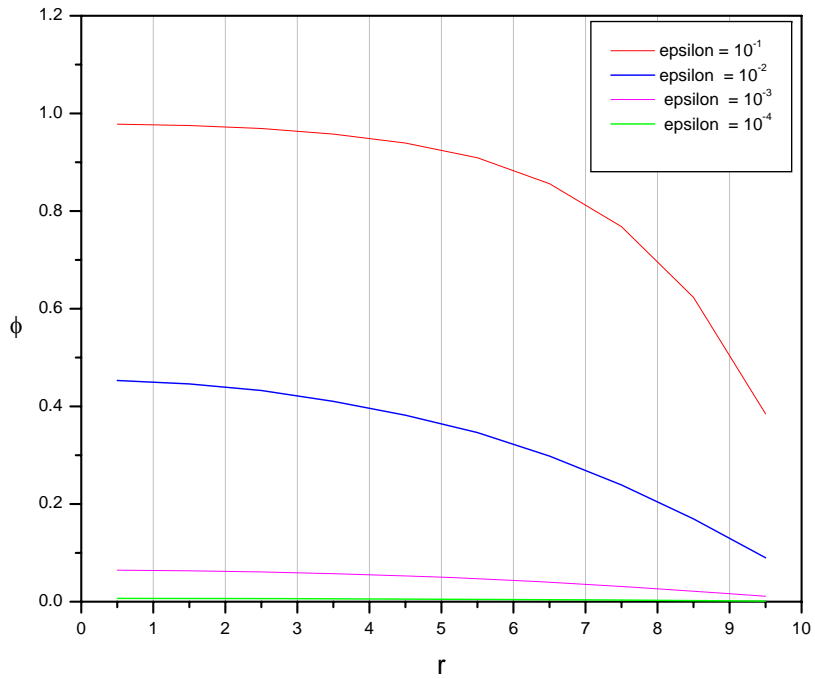Figure 5.16: Problem 5. The cell-average scalar flux for CMLC.

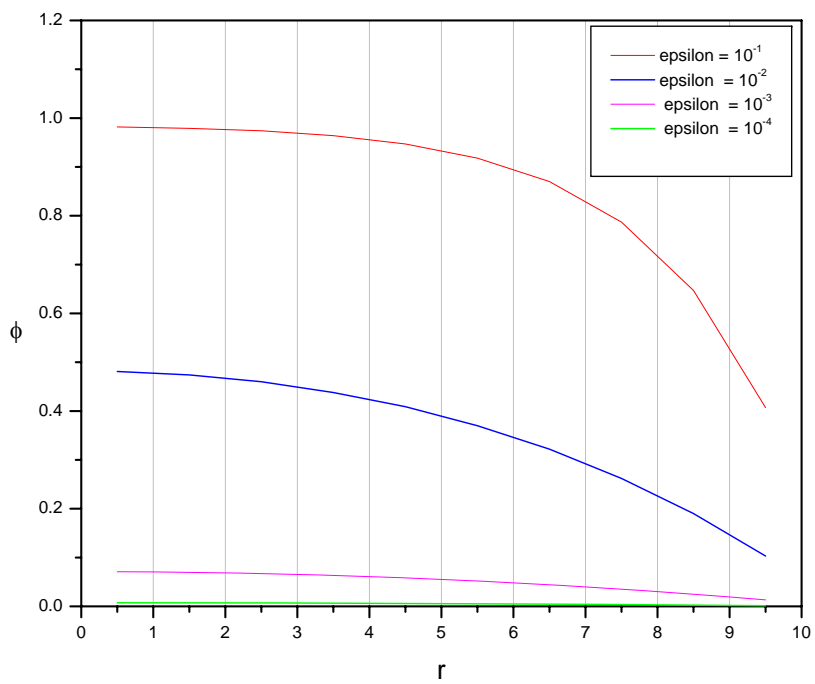Figure 5.17: Problem 5. The cell-average scalar flux for LCMSC.

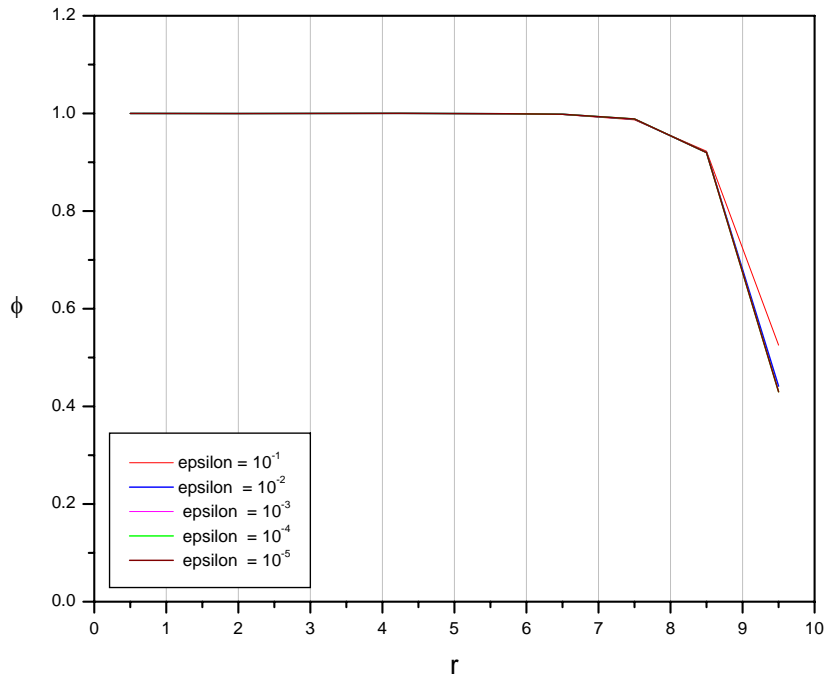Figure 5.18: Problem 5. The cell-average scalar flux for SLCMSC.

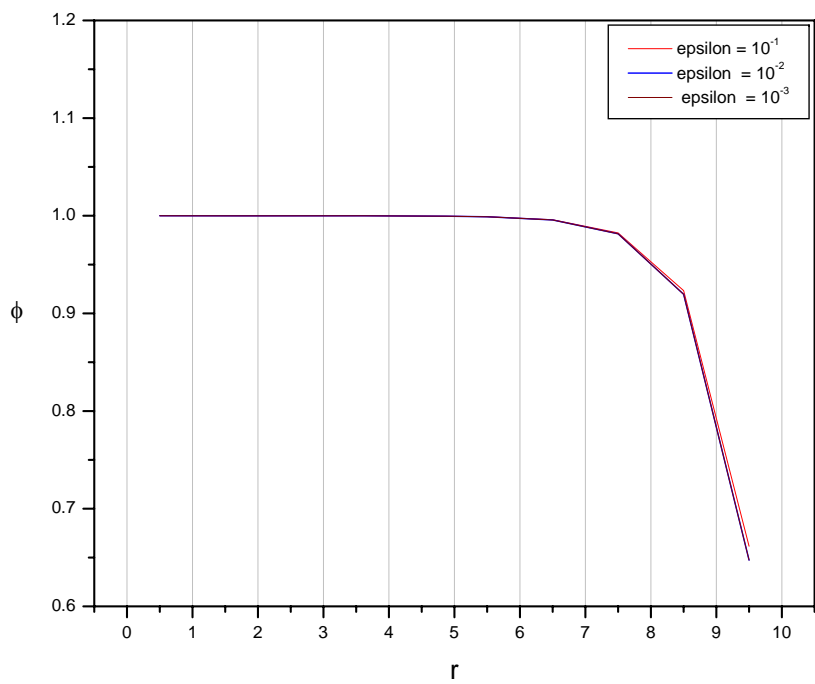Figure 5.19: Problem 5. The cell-average scalar flux for LLCM.

Figure 5.20: Problem 5. The cell-average scalar flux for ESLC.

Chapter 6

CONCLUSION

The goal of this research is to develop a family of characteristic methods for transport problems in 1-D spherical geometry that produce accurate solutions in the asymptotic diffusion limit. The primary motivations behind this work are science and engineering applications that require radiative transfer solutions for problems that have optically thick and diffusive regions. The transport methods developed in this paper are vertex-based methods of characteristics. The two variants of VMOC, linear and parabolic interpolation of the total source term, were analyzed for their performance in the thick diffusion limit. The analysis showed that neither of these methods limit to an accurate discretization of the diffusion equation nor did they generate the appropriate boundary conditions. Numerical results of problems were presented and confirm that VMOC have an unphysical behavior for problems with diffusive regions.

We have derived the conservative versions of vertex-based method of characteristics, based on ideas posed in [14], for long and short characteristics along with a Long Linear

Characteristic method and the Explicit Slope Long Characteristic method. The asymptotic analysis for CMLC, SLCMLC, and LLCM was performed. Numerical results confirmed the analysis for CMLC and SLCMLC. For the LLCM case, our results show that this method does limit to a discretized version of the diffusion equation. We have yet to confirm the boundary condition and therefore did not present results for the unresolved boundary layer test. Lastly, ESLC was not analyzed but gave numerical results similar to those found in the slab geometry counterpart [20]. We found that ESLC generates a solution that is accurate for diffusive problems without unresolved boundary layers. For problems that exibit large changes in the scattering ratio across material interfaces, a slope limiter is needed to improve the performance of ESLC.

Future work will involve finishing the asymptotic analysis of ESLC and completing the numerical results for LLCM. This will allow for continued development of advanced conservative methods of characteristics with better properties for 1D cylindrical and 2D curvilinear geometries.

BIBLIOGRAPHY

[1] R.D. RICHTMYER, "**Difference Methods for Initial-Value Problems**, Interscience Publishers, INC., New York, (1957).

[2] G.I. MARCHUK, "**Numerical Methods for Nuclear Reactor Calculations**," Chapman & Hall, **12**, 231 (1959).

[3] V.S. VLADIMIROV, "Numerical Solution of the Kinetic Equation for a Sphere," *Comp. Math.,* **3**, 3 (1958) (in Russian).

[4] S. CHANDRASEKHAS, **Radiative Transfer**, Dover Publications, New York (1960).

[5] V.YA. GOL'DIN, "Characteristic Difference Scheme for Non-Stationary Kinetic Equation," *Soviet Mathematics - Doklady*, **1**, 902 (1960).

[6] V.YA. GOL'DIN, N.N. KALITKIN , and T.V. SHISHOVA, "Nonlinear Difference Schemes for Hyperbolic Equations," *USSR Comp. Math. and Math. Phys.* **5**, 229 (1968).

[7] K. TAKEUCHI, "A Numerical Method for Solving the Neutron Transport Equation in Finite Cylindrical Geometry," *J. Nucl. Sci.,* **6**, 446 (1969).

[8] A.V. NIKOFOROVA, V.A. TARASOV, and V.E TROSHCHIEV, "Solutions of the Kinetic Equations by the Divergent Method of Characteristics," *USSR Comp. Math. and Math. Phys.*, **12**, 251 (1972).

[9] W.H. REED, "The Effectiveness of Acceleration Techniques for Iterative Methods in Transport Theory", *Nucl. Sci. Engr.*, **45**, 245 (1971)

[10] J.R. ASKEW, "A Characteristic Formulation of the Neutron Transport Equation in Complicated Geometries," Winfrith Report M1108, Atomic Energy Establishment (1972).

[11] E.W.LARSEN and J.B.KELLER, "Asymptotic solution of Neutron Transport Problems for Several Mean Free Paths," *J. Math. Phys.,***15**, 75 (1979)

[12] J.E. MOREL and K.W. MONTRY, "Analysis and Elimination of the Discrete-Ordinates Flux Dip," *Trans. Theory Stat. Phys.*, **13**, 615 (1984).

[13] E.E LEWIS and W.F. MILLER,JR., "**Computational Methods of Neutron Trasnport**," Wiley-Interscience, New York (1994).

[14] D.Y. ANISTRATOV AND V.YA. GOL'DIN, "Comparison of Difference Schemes for the Quasi-Diffusion Method for Solving the Transport Equation," *Problems of Atomic Sci. and Eng: Methods and Codes for Numerical Solution of Math. Physics Problems*, **2**, 17 (1986) (in Russian).

[15] E.W. LARSEN AND J.E. MOREL, "Asymptotic Solutions of Numerical Transport Problems in Optically Thick Diffusive Regimes II," *J. Comput. Phys.*, **83**, 212 (1989).

[16] E.W.LARSON, "Asymptotic Diffusion Limit of Discretized Transport Problems," *Nucl. Sci. Engr.*, **112**, 336 (1992).

[17] T.S PALMER and M.L. ADAMS, "Curvilinear Geometry Transport Discretizations in the Thick Diffusion Limit, *Proc. International Conf. on Mathematical Methods and Supercomputing in Nuclear Applications*, April 19-23, 1993, Karlsrhe, Germany, **1**, 33 (1993).

[18] M.L. ADAMS, T.A. WAREING and W.F. WALTERS, "Characteristic Methods in Thick Diffusive Problems," *Nucl. Sci. Engr.*, **130**, 18 (1998).

[19] K.D. LATHROP, "A Comparison of Angular Difference Schemes for One-Dimensional Spherical Geometry S_n Equations," *Nucl. Sci. Engr.*, **134**, 264 (1998).

[20] H.L. HANSHAW and E.W. LARSEN, "The Explicit Slope S_N Discretization Method," *Nucl. Math. and Comp. Sci.: A Century in Review, A Century A new*, Gatlinburg, Tennessee, April 6-11,2003, American Nuclear Society,La Grange Park, IL (2003).

[21] J.S. WARSA and J.E. MOREL, "Solution Algorithms For a P_{N-1} Equivalent S_N Angular Discretization of The Transport Equation In OneDimensional Spherical Coordinates," *Proc. Joint Int. Topl. Mtg. Mathematics and Computations and Supercomputing in Nuclear Applications*, Monterey, California, April 15-19, 2007, American Nuclear Society (2007).

[22] D.Y. ANISTRATOV and J.T. FLEMING, "Asymptotic Diffusion Analysis of Conser-

vative Methods of Long and Short Characteristics for 1D Spherical Geometry," *Trans. Am. Nuc. Soc.*, **98**, 504 (2008).

[23] M.E. RISING and T.S. PALMER, "Momoent-Based Versions of the Spherical Geometry Method of Tubes in Thick, Diffusive Regions," *Nucl. Sci. Engr.*, **160**, 284 (2008).